



PERGAMON

Progress in Biophysics & Molecular Biology 72 (1999) 367–405

Progress in
Biophysics
& Molecular
Biology

www.elsevier.com/locate/pbiomolbio

Structure and dynamics of membrane proteins as studied by infrared spectroscopy

José Luis R. Arrondo^{a, b, *}, Félix M. Goñi^{a, b}

^aUnidad de Biofísica (Centro Mixto CSIC - UPV/EHU), Bilbao, Spain

^bDepartamento de Bioquímica, Universidad del País Vasco, P.O. Box 644, E-48080 Bilbao, Spain

Received 19 April 1999

Abstract

Infrared (IR) spectroscopy is a useful technique in the study of protein conformation and dynamics. The possibilities of the technique become apparent specially when applied to large proteins in turbid suspensions, as is often the case with membrane proteins. The present review describes the applications of IR spectroscopy to the study of membrane proteins, with an emphasis on recent work and on spectra recorded in the transmission mode, rather than using reflectance techniques. Data treatment procedures are discussed, including band analysis and difference spectroscopy methods. A technique for the analysis of protein secondary and tertiary structures that combines band analysis by curve-fitting of original spectra with protein thermal denaturation is described in detail. The assignment of IR protein bands in H₂O and in D₂O, one of the more difficult points in protein IR spectroscopy, is also reviewed, including some cases of unclear assignments such as loops, β -hairpins, or 3_{10} -helices. The review includes monographic studies of some membrane proteins whose structure and function have been analysed in detail by IR spectroscopy. Special emphasis has been made on the role of subunit III in cytochrome *c* oxidase structure, and the proton pathways across this molecule, on the topology and functional cycle of sarcoplasmic reticulum Ca²⁺-ATPase, and on the role of lipids in determining the structure of the nicotinic acetylcholine receptor. In addition, shorter descriptions of retinal proteins and references to other membrane proteins that have been studied less extensively are also included. © 1999 Elsevier Science Ltd. All rights reserved.

Keywords: Infrared spectroscopy; Membrane proteins; Band analysis; Difference spectroscopy; Structure-function relationship

* Corresponding author. Tel.: +34-946-012-625; fax: +34-944-648-500.

E-mail address: gbproarj@lg.ehu.es (J.L.R. Arrondo)

1. Introduction

An understanding of cell membranes implies the study of biological structures of great complexity and important functions. Chief among them are the proteins. Membrane proteins exist in a variety of sizes and shapes. Some of the so-called intrinsic or integral proteins span the lipid bilayer and, while being stabilised mainly by hydrophobic interactions within the hydrocarbon lipid matrix, they keep contact with the aqueous medium at both sides. Extrinsic membrane proteins bind to the polar region of a single phospholipid leaflet and establish mainly electrostatic interactions with the lipid component and/or with other proteins. In this review, only the intrinsic proteins will be considered because, from the structural point of view, little if any difference can be found between extrinsic and soluble proteins. The structural differences between membrane and soluble globular proteins are not only a consequence of their different environments, but they reflect as well the varying mechanisms responsible for their folding and assembly.

The properties of membrane proteins make difficult the use of structural techniques to study their conformation. Thus, even if X-ray crystallography is the method of choice for detailed protein structure analysis, obtaining three-dimensional crystals of membrane proteins is not easy. To date, the number of different membrane proteins that have been crystallised is no bigger than fifteen. Two-dimensional crystals can also be used to produce a three-dimensional picture of the protein, but to a lower resolution. Nuclear magnetic resonance (NMR) spectroscopy offers an appropriate alternative to X-ray crystallography for obtaining detailed three-dimensional structures, but at least in its present state it is limited to proteins of molecular weight lower than those usually found in membranes.

It should also be noted that obtention of a protein structure does not immediately make clear its molecular mechanism. For example, in a protein with an enzymatic activity, this would imply the knowledge of the interactions of substrate, intermediate(s) and product with amino acid side chains in the 'active centre', that sometimes cannot be solved in a unique way within a given structure. In many aspects of protein structure and function, therefore, there is a need for complementary, lower resolution techniques that can provide useful information, even in proteins with known three-dimensional structures.

Infrared spectroscopy is useful, either as an alternative option or as a complement to the high-resolution techniques in membrane protein studies, because of the wealth of information provided. Furthermore, the lipid environment does not perturb the resolution or sensitivity of the spectra and can also be the object of simultaneous study, thus providing information on the lipid-protein interactions. Although infrared spectroscopy was first applied to proteins as early as in 1952 (Sutherland, 1952) before any detailed X-ray results were available, its use in membrane proteins or in proteins in physiological environments in general has only been possible after the revolution in instrumentation produced by instruments based on the Michelson interferometer and the fast Fourier transform. The increase in signal-to-noise ratio obtained with these instruments allows the subtraction of the aqueous buffer, thus obtaining spectra whose bands contain information on the protein in its native environment, and are free from spectral interference by the solvent. In principle, a structure as large as a protein would give rise to an enormous number of overlapping vibrational modes obscuring the information

that could be obtained in practice, but because of the repeating patterns of the biological molecules, e.g. the secondary structure of the protein backbone, the spectra are much simpler and useful structural information can be obtained.

Structural analysis usually implies a mathematical approach used to extract information contained in the composite bands, designated in IR spectroscopy as ‘amide bands’, obtained from proteins. Commonly used methods of analysis imply narrowing the intrinsic bandwidths to visualise the overlapping band components and then decomposing the original band contour into these components by means of an iterative process. The various components are finally assigned to protein or subunit structural features. A different approach consists of the use of infrared spectroscopy to examine ligand-induced changes produced in proteins during their functional cycles. The strategy used is called ‘difference infrared spectroscopy’ and consists of looking closely at the bands corresponding to protein or ligand groups that undergo changes during the transition from one state to another. By these means it is possible to detect changes in a single amino acid residue. In order to perform the assignment correctly it is necessary to obtain spectra with a signal-to-noise ratio better than 10^4 . In addition, a proper assignment may require the preparation of specific mutant proteins. Also, for the study of some protein functions, the functional substates must be long enough to be measured, and time-resolved difference spectroscopy techniques have been developed to this aim.

The increased sensitivity of modern infrared spectrometers has also allowed the use of sampling techniques other than transmission. Thus reflection techniques, and particularly attenuated total reflectance (ATR), have been applied to study structural aspects of membrane proteins and to measure the orientation of membrane components through the use of polarized IR radiation. This sampling technique was developed by Harrick (1967) and later applied to membranes by Fringeli (Fringeli and Günthard, 1981). Various recent reviews have been published on the use of ATR in studying membrane protein structure and orientation (Goormaghtigh and Ruyschaert, 1990; Axelsen and Citra, 1996; Tamm and Tatulian, 1997). Other sampling techniques with potential application to biomembranes, such as infrared microscopy, have not yet succeeded in providing useful data on membrane protein structure and function. Infrared imaging visualizes the lipid and protein content of the cells and can be of great interest in the future (Lewis et al., 1997; Colarusso et al., 1998).

The present review deals with the study of membrane protein structure and function using either IR band analysis or difference IR spectroscopy. We have focussed our attention specially on proteins, e.g. cytochrome *c* oxidase, Ca^{2+} -ATPase or the nicotinic acetylcholine receptor, for which a significant collection of IR data exists. Conversely, less attention is being paid to extensively studied proteins, e.g. retinal proteins, but about whom there are yet many unanswered questions even after different structures at 2–3 Å resolution have been published. Also, publications devoted to the prosthetic groups of proteins, rather than to the peptide chain components will not be included in our study; the interested reader may refer to Section II of the book edited by Carmona et al. (1997). Recently, several reviews dealing with IR studies on different aspects of membrane protein structure/function or on protein orientation have been published (Goormaghtigh et al., 1994b; Siebert, 1995; Axelsen and Citra, 1996; Haris et al., 1996; Tamm and Tatulian, 1997). Our former review in this journal (Arrondo et al., 1993) can be consulted for the more basic aspects, or for the less recent, yet relevant literature.

2. Data treatment

The structural information contained in the infrared bands of a protein spectrum can be retrieved from the so-called amide bands, and particularly from the amide I band. Alternatively, the difference spectrum between two states of the protein can be studied.

2.1. Band analysis

Most methods concentrate on the analysis of the amide I band, located between 1700 and 1600 cm^{-1} and composed mainly ($\approx 80\%$) by the C=O stretching vibration of the peptidic bond. The band can be analysed by comparison with a ‘calibration set’ of spectra of proteins with known structure, what is called ‘factor analysis’, or else by decomposing the amide I band into its constituents by curve-fitting.

2.1.1. Methods based on calibration sets

Information on protein secondary structure has been obtained by comparing the infrared spectrum of an unknown protein with a set of spectra from proteins with known X-ray structure. The approach is similar to those used in circular dichroism and involves obtaining ‘pure component spectra’ for each conformation, and then treating the unknown protein as a mixture of the ‘pure spectra’ (for a review see Bandekar, 1992; Goormaghtigh et al., 1994b; Arrondo et al., 1993). The methods developed for that purpose include partial least squares (PLS) (Dousseau and Pezolet, 1990), and factor analysis (Lee et al., 1990; Baumruk et al., 1996). An improved approach using 2D correlation maps for analysis of a series of spectra of proteins has also been developed (Pancoska et al., 1999). The major difficulty encountered in applying these methods to membrane proteins is finding an appropriate set of relevant reference proteins. A report using factor analysis has been applied with membrane proteins as models (Corbalán-García et al., 1994) widening the field of application of the procedure. Once the suitable calibration set has been found, this quantification method provides a quick and easy way for obtaining major conformational features, i.e. α -helix, β -sheet, etc. of the protein secondary structure. A disadvantage of the method is that only part of the information contained in an infrared spectrum is used, i.e. the one for whom a ‘correlate’ in the set of pure component spectra is found.

2.1.2. Methods based on curve-fitting

Curve-fitting includes the decomposition of the amide I band into its constituents and the assignment of these components to protein structural features. To start the quantification process, the number and position of the bands and a rough estimation of bandshapes, widths and heights of the components is needed. These initial parameters are then left to iterate, using programs based on a combination of Gaussian and Lorentzian (or Cauchy) functions. Curve-fitting is best performed on original bands, although it is sometimes accomplished, less accurately, on more shapely spectra obtained through deconvolution or derivation.

2.1.2.1. Original spectra. The information originated from the infrared absorption of all the peptide groupings is contained in the envelope of the amide I band. However, retrieving this information is not a straightforward process. As can be seen in Fig. 1, this IR band is shapeless because of the overlapping of its constituents, and the number and position of component bands can only be obtained through deconvolution or derivation (Arrondo et al., 1993). Moreover, the amide I band can exhibit variations in baseline, due to instrumental problems or to solvent subtraction. All these contribute to decreasing the accuracy of the measurements. In order to study minor effects produced by ligand binding or a variety of physical or chemical agents upon protein structure or stability, we have devised a method that combines curve-fitting with the gradual induction of a conformational change in the protein, through carefully regulated temperature variations.

This method analyses series of spectra obtained in H₂O and D₂O while heating the sample from room temperature until thermal denaturation is accomplished. A picture of the protein before and after denaturation can be seen in Fig. 2. In that case, corresponding to sarcoplasmic reticulum from rabbit muscle in H₂O and D₂O buffers, the denaturation pattern is indicated by the appearance of two characteristic bands at around 1627 and 1693 cm⁻¹ in H₂O and around 1620 and 1685 cm⁻¹ in D₂O, due to protein aggregation. The amide II band is also affected by the denaturation process. The curve-fitting procedure is as follows: the

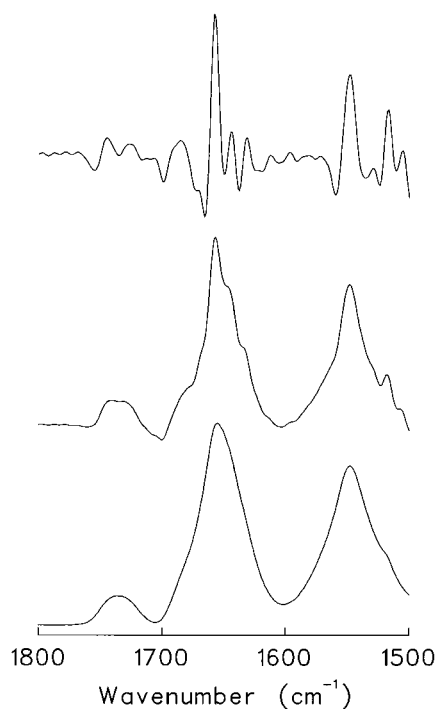


Fig. 1. Infrared spectrum in the 1800–1500 cm⁻¹ region of sarcoplasmic reticulum in H₂O medium. Original spectra obtained after subtracting (Arrondo et al., 1994) the solvent contribution (lower trace), deconvolved spectra using a bandwidth (FWHM) of 18 cm⁻¹ and a *k* of 2 (medium trace) and Fourier derivative using a power of 3 and a breakpoint of 0.3 (upper trace).

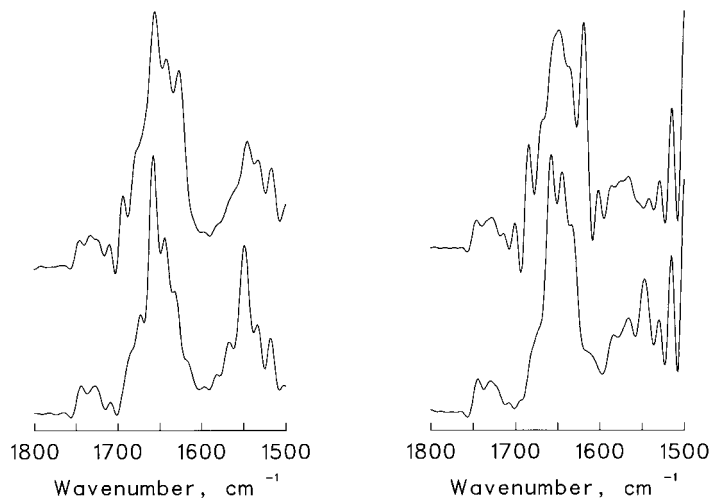


Fig. 2. Deconvolved spectra of sarcoplasmic reticulum in H₂O (left panel) or D₂O (right panel) medium at room temperature (lower traces) or after thermal denaturation (upper traces). The parameters used for deconvolution were a FWHH of 18 cm⁻¹ and a k of 2.5.

number and position of bands is obtained from the deconvolved (bandwidth=18 and $k = 2$) and the Fourier derivative (power=3 and breakpoint=0.3) spectra. The baseline is removed before starting the fitting procedure and initial heights are set at 90% of those in the original spectrum for the bands in the wings and for the most intense component, and at 70% of the original intensity for the other bands. An iterative process follows, in two stages. (i) The band position of the component bands is fixed, allowing widths and heights to approach final values; (ii) band positions are left to change. For bandshape a combination of Gaussian and Lorentzian functions is used in principle. The restrictions in the iterative procedure are needed because initial width and height parameters can be far away from the final result due to the overlapping of bands, so that spurious results can be produced.

In such a way, information from band position, percentage of amide I band area and bandwidth are obtained for every component. Band position reflects the conformation of the structural element under study (i.e. α -helix, β -sheet, and so on). From the canonical band positions as discussed e.g. in Susi (1969), it can be inferred that only large changes (≥ 10 cm⁻¹) in band position indicate variations in the secondary structure, whereas smaller shifts (≤ 6 cm⁻¹) reflect local changes in a given conformation. The integrated intensity of each component, usually expressed as percent band area, can be related to the proportion of protein in that particular conformation, assuming that the molar absorptivities of the different component bands are alike (De Jongh et al., 1996; Chehin et al., 1999). Finally, the width-at-half-height (often expressed as bandwidth) can be related to the freedom of movement of the structure associated to that particular component, although a large difference in band area can also influence its width (Arrondo et al., 1994). Fig. 3 shows the plots of wavenumbers as a function of temperature. The dispersion of the experimental points for a given conformation (band position) provides an estimation of the error in percentage area quantification. Using an average band position as a starting point to perform a second curve-fitting reduces

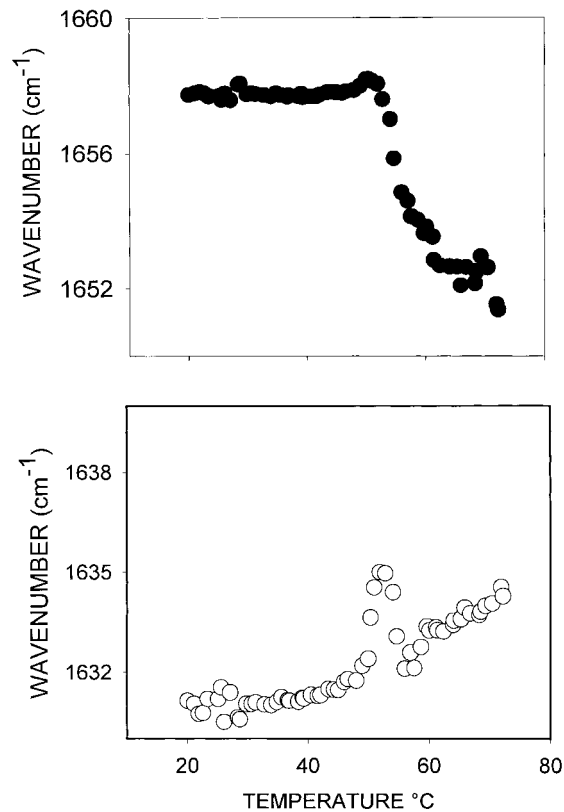


Fig. 3. Thermal profiles of the amide I band of sarcoplasmic reticulum Ca^{2+} -ATPase components at 1657 cm^{-1} corresponding to α -helix (●), and 1632 cm^{-1} corresponding to β -sheet (○). See Section 4.2 for details.

considerably the experimental error, thus allowing the detection of small changes in protein conformation.

2.1.2.2. Resolution-enhanced spectra. Curve-fitting methods based on the use of deconvolved spectra use these more shapely spectra to overcome the problems encountered in decomposing the original amide I. The fitting is then simplified, and information on band position and percentage band area is obtained. The method was developed by Byler and Susi (1986) (for a review see Bandekar, 1992; Arrondo et al., 1993; Goormaghtigh et al., 1994b). The assumptions are implicit that the bandwidths of all the components are alike and that the Lorentzian component of the original amide I envelope is well known, to avoid over- or under-deconvolution (Pierce et al., 1990). A method using second derivative spectra to quantify protein structure has also been described (Kennedy et al., 1991). This method assigns different amide I regions to secondary structures according to a comparison with a set of 12 proteins of known X-ray structure (Dong et al., 1990). In principle, derivation produces faster spectral degradation than deconvolution, therefore the information can be partially lost (Cameron and Moffat, 1984; Cameron and Moffat, 1986). An assessment of the different methods using artificial curves constructed with parameters corresponding to cytochrome *c* oxidase shows that the use of

resolution enhanced spectra is less reliable than the analysis of original spectra (Echabe and Arrondo, 1997). An additional study using deconvolved spectra and protein secondary structure prediction with factor analysis-based restricted multiple regression using a set of 23 proteins dissolved in H₂O found that the prediction quality varied depending on the deconvolution parameters used (Wi et al., 1998).

2.1.2.3. Linked analysis. This novel procedure for IR band fitting has been recently introduced by Silvestro and Axelsen (1999). Linked analysis was previously developed for the global analysis of multiexponential fluorescence intensity decays. The method allows the simultaneous fit of multiple bands. Also parameters in different spectra may be linked (i.e. shared or constrained to the same value). This has been applied to the simultaneous fitting of spectra collected with different polarizer orientations wherein only amplitude changes are expected, while position, width and shape of the component bands should remain invariant. In this way subjectivity in spectral analysis is reduced, and the overall reliability is improved.

2.2. Difference spectroscopy

The most obvious application of difference spectroscopy to protein studies is the removal of the strong absorbing solvent band. However, the importance acquired by the dynamic studies is such that the term difference spectroscopy is usually applied to the difference between two spectra acquired in two different states of a protein reaction or of a conformational change (for a review see Mäntele, 1993; Siebert, 1995). In principle, the difference spectrum should be obtained by subtraction of the buffer-subtracted protein spectra in state 1 minus state 2. However, because of the very low absorbance that has to be measured (the absorbance of a single peptidic bond can be in the order of 10^{-5} absorbance units), the variations produced by the change of sample in the spectrometer or the buffer removal (buffer absorbance being in the order of 1 absorbance unit) would make this approach valid only for low molecular weight samples, in which less bonds are involved, or for conformational changes involving at least 2–3% of the bonds. Thus, difference spectroscopy has been used most often in reactions that can be triggered inside the measuring cell. A reaction between an initial and a final state is produced, a succession of spectra recorded and the difference between spectra (as a ratio of single beam traces) measured. The changes produced even at the level of a single bond can then be compared. The method allows not only the measurement of the difference between the final and initial states, but also the following of the reaction time course in the time-resolved difference spectroscopy. The reaction trigger should not disturb the sample or otherwise interfere, apart from specifically and quantitatively starting the desired reaction. The first trigger used was light in light-sensitive proteins and light minus dark difference spectra were obtained in the early 1980s for bacteriorhodopsin, the visual pigment rhodopsin or the photosynthetic reaction centres from plants and bacteria (Mäntele, 1993). Photoreactive haem proteins were also studied by the same procedure (Dong and Caughey, 1994). Later, light was used as a trigger to liberate a caged substrate and initiate a reaction. This was first applied to study the difference between the E₁ and E₂ states of the sarcoplasmic reticulum Ca²⁺-ATPase (Barth et al., 1990), and more recently a number of cages have been developed to study different reactions (for a review see Cepus et al., 1998). An additional way of triggering

reactions to obtain difference spectra is the use of ultra-thin-layer electrochemical cells which allow redox reactions of proteins to be triggered on transparent electrodes. The redox reactions that can be studied in membranes include a large number of proteins and the method has been extensively used to study the mechanism of cytochrome *c* oxidase. This kind of difference spectroscopy has also been termed ‘reaction-induced difference spectroscopy’ (Mäntele, 1993).

The use of mutants and isotope labelling has contributed to overcome the problem of assignment in difference spectroscopy. In principle, infrared bands should be assigned to the vibrational modes of a molecule by performing a normal mode calculation and matching the results, what is not feasible in an entire protein. Even if group frequencies are assumed, the overcrowding of bands that can be obtained and the differences in band position due to interactions with other molecules make this assignment, as in band-fitting, a non-straightforward process. Isotope labelling produces a change in band position caused by the difference in reduced mass that allows the discrimination between molecules of the same kind or the allocation of a band variation to a particular amino acid. Genetic engineering has also helped in the assignment of specific bands in the difference spectrum, especially when the corresponding high-resolution structure has been solved. Specific questions about the role of an amino acid in the mechanism of a protein can be asked by designing proteins where that particular amino acid has been changed.

3. Band assignment

A protein conformation can be defined by a set of dihedral angles ϕ_i and ψ_i and by the short- or long-range interactions between different peptide groups, i.e. hydrogen bonding. The relationship between conformation and band position can be studied using the following relationship (Susi, 1969; Fringeli and Günthard, 1981):

$$\left[\nu(\delta, \delta') = \nu_0 + \sum_i D_j \cos(j\delta) + \sum_j D'_j \cos(j\delta'), \right] \quad (1)$$

where the first term ν_0 corresponds to the unperturbed amide frequency, δ and δ' are the phase angles (0 or π) between adjacent groups in the same chain or in the neighbouring chain connected by a hydrogen bond, D_j and D'_j are coupling constants corresponding to the intrachain or interchain interactions.

Equation (1) can describe in principle the splitting and polarization of the amide I band in different conformations (Susi, 1969). However, it does not furnish direct information concerning numerical frequency values or relative intensities. Some modes might be so weak as to be practically unobservable. Others might overlap, resulting in odd-shaped bands with apparently ill-defined absorption maxima. Additional information can also be obtained from polarization measurements (for a review, see Goormaghtigh and Ruyschaert, 1990; Tamm and Tatulian, 1997). More refined approaches, such as the transition dipole coupling (Krimm and Bandekar, 1986), the three-doorway state (Torii and Tasumi, 1992a,b) or the transfer of Cartesian molecular force field and electric property tensors from smaller molecules or fragments of a large molecule to estimate the force fields of the large system (Bour et al., 1997)

have also been developed. The relationship between normal modes and final bandshapes has also been shown (Krimm and Reisdorf, 1994).

3.1. Studies in aqueous solution

The considerations of the preceding paragraph refer mostly to solid samples. However, under physiological conditions, proteins occur in aqueous solution, where the refractive index of the solvent, specific solvent-solute interactions and spectroscopic interference by solvent bands contribute to increase the difficulty of the amide I band analysis. Solvent interference is particularly disturbing since the strong HOH bending mode around 1643 cm^{-1} practically coincides with the amide I band. One way of circumventing this difficulty is to study proteins in D_2O solutions. The amide I' band (i.e. the analogous amide I band in D_2O) is easily observed, whereas the amide II' is obscured by the absorption of trace amounts of HOD and the CH_2 bending of the lipid moiety in membrane proteins. The influence of deuteration on each protein conformation will be discussed later, the most prominent feature being a shift in some of the components. The main problem of using D_2O arises from the possibility of protein denaturation during the $\text{H}_2\text{O} \rightarrow \text{D}_2\text{O}$ substitution treatment (Rial et al., 1990) or from an incomplete deuteration that could give rise to overlapping bands and alter bandshape. Incomplete deuteration is a common feature in membrane proteins (Earnest et al., 1990; Arrondo et al., 1994). In principle, the amide I and amide I' bands of a protein must possess the same conformational information and thus the study of a protein in both media helps to extract this information. A method using different degrees of deuteration to obtain a more refined quantification procedure using factor analysis has recently been presented (Baello et al., 1999). Fig. 4 shows the spectrum of cytochrome *c* oxidase in H_2O and D_2O media in which the differences in the amide I bandshape and the incomplete deuteration can be observed.

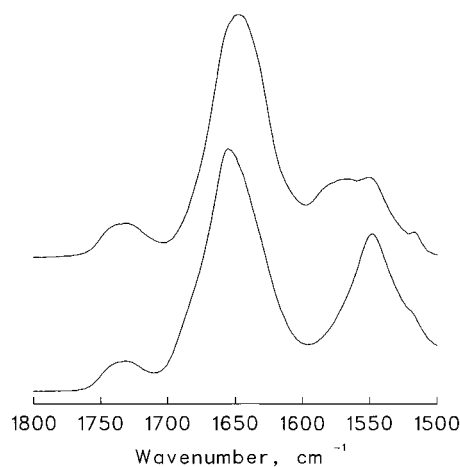


Fig. 4. Infrared spectra of the $1800\text{--}1500\text{ cm}^{-1}$ region corresponding to the amide I and II bands in H_2O medium (lower trace) and amide I' and the residual amide II in D_2O medium (upper trace) of Ca^{2+} -ATPase from sarcoplasmic reticulum.

3.2. Helical structures

The infrared spectrum of α -helix has been studied using different approaches. Homopolypeptides or proteins whose α -helical structure was known from X-ray diffraction have been studied, and values of 1652 cm^{-1} in H_2O and 1650 cm^{-1} in D_2O are accepted for the $\nu(0)$ mode, although values of 1655 cm^{-1} and 1658 cm^{-1} have also been obtained solving Eq. (1) (Krimm and Bandekar, 1986). In H_2O the α -helix band overlaps with the signal arising from unordered structure, but these two bands can be resolved in D_2O . The assignment of α -helix to bands in the region $1648\text{--}1658\text{ cm}^{-1}$ is generally admitted (Arrondo et al., 1993). However, some exceptions to this assignment have been described. Bacteriorhodopsin, a helical protein, exhibits a band at 1660 cm^{-1} that has been attributed to α_{II} -helix, a structure with different dihedral angles, but the same number of residues per turn and unit axial translation (Krimm and Dwivedi, 1982). Some peptides expected to have an α -helix structure have been reported to exhibit in D_2O a band around 1641 cm^{-1} , outside the limits assigned to this structure (Susi, 1969; Jackson et al., 1989; Flach et al., 1994). The shift may be produced by a change in the geometry of the α -helix that was described for some polyaminoacids (Tomita et al., 1962). Even if an effect of sample preparation can be at the origin of this abnormal shift induced by deuteration, these reports reinforce the need of obtaining the spectra in both solvents to avoid misinterpretation of the results. More recently, it has been found that coiled coils can give rise to several bands due to helix-helix coupling, including one around 1641 cm^{-1} (Reisdorf and Krimm, 1996).

An additional helical structure that has attracted considerable interest is the 3_{10} -helix. Different reports gave values for the position of this band at either around 1660 cm^{-1} (Kennedy et al., 1991) or near 1645 cm^{-1} (Miick et al., 1992). However, another report seems to point to a relationship between band position and length for this helix (Reisdorf and Krimm, 1994). Thus, short 3_{10} helices would appear around 1660 cm^{-1} and longer segments would have their signals displaced to lower wavenumbers.

3.3. Extended structures

The most common extended structure found in proteins is the antiparallel β -sheet. Equation (1) has two solutions for this structure, one at low frequency [$\nu(0, \pi)$], around 1630 cm^{-1} , and one at high frequency [$\nu(\pi, 0)$], that appears at 1690 cm^{-1} in H_2O medium and at 1675 cm^{-1} in D_2O medium. Parallel β -sheet also gives rise to the same low frequency band; in principle, the high frequency signal should appear around 1648 cm^{-1} , but unfortunately the parallel β -sheet is poorly characterized (Susi and Byler, 1987; Castresana et al., 1988b). The relationship between the integrated intensities of the high and low frequency components of the β -sheet signal presents also some difficulties. It can be predicted that the high frequency component intensity is less than 1/10th of that of the low frequency band (Fraser and MacRae, 1973, so that the contribution of the high frequency band becomes negligible in proteins not possessing high amounts of β -sheet. Moreover, the appearance of a band due to β -turns at a similar frequency in D_2O medium (Krimm and Bandekar, 1986), increases the uncertainty of this assignment.

Bands at frequencies lower than 1630 cm^{-1} were first described for extended chains in polylysine (Susi, 1969) and attributed to antiparallel-chain pleated sheet. They were also found

in denatured proteins in D₂O buffer (Muga et al., 1993; Naumann et al., 1993). However, they are not common in native proteins neither in H₂O nor in D₂O. In native proteins, a band at a wavenumber lower than 1630 cm⁻¹ was first found in concanavalin A (Alvarez et al., 1987; Arrondo et al., 1988) and assigned to peptides in an extended configuration, with a hydrogen-bonding pattern formed by peptide residues not taking part in intramolecular β -sheet but rather hydrogen-bonded to other molecular structures, e.g. forming intermolecular hydrogen bonding in monomer–monomer interaction. This kind of signal was also found in triose phosphate isomerase (Castresana et al., 1988b) where the β -sheet would be hydrogen-bonded to the α -helix, and even at a lower frequency in human low density lipoproteins, where it was assigned to ‘low frequency β -sheets’ (Goormaghtigh et al., 1989 or to a β -structure less accessible to the external solution (Herzyk et al., 1987). We called this pattern ‘ β -edge’ as typical of the outer strands of β -sheets (Castresana et al., 1988a; Arrondo et al., 1989); it also implies intermolecular hydrogen bonding, as postulated for the low frequency bands in irreversibly aggregated proteins (Surewicz et al., 1990; Jackson et al., 1991) or in monomer–monomer contacts, as in concanavalin A (Arrondo et al., 1988). Bands around 1620 and 1693 cm⁻¹ in H₂O and D₂O (without isotopic shift) have been found in a peptide forming a β -hairpin (Arrondo et al., 1996), and they have also been detected in proteins possessing β -sheet structure and β -hairpins with specific turns that give rise to more rigid structures (Chehin et al., 1999).

3.4. Turns and loops

The β -turn is characterized by the presence of a hydrogen bond between amino acid residues ($i \rightarrow i+3$). Different types of β -turns have been characterized in proteins (Richardson, 1981), and their infrared behaviour studied (Krimm and Bandekar, 1986). However, because of the difficulty in analyzing the intensities there is no clear assignment of the amide I band components for the different kinds of β -turns, and the various bands appearing between 1660 and 1700 cm⁻¹ are assigned to turns in a nonspecific way.

A band around 1645 cm⁻¹ in H₂O medium was observed in streptokinase (Fabian et al., 1992), and attributed to ‘open loops’, i.e. fully hydrated loops, not interacting with nearby amide functional groups. The assignment of this frequency to loops was confirmed by the study of a membrane-unrelated lectin composed of β -sheets, turns and loops (Chehin et al., 1999). This assignment is not unambiguous, because other structures also give rise to bands in this spectral region. It is to be expected that in membrane proteins loops will be among the structures emerging from the bilayer, and giving rise to bands in the 1645 cm⁻¹ region.

3.5. Unordered structures

According to Eq. (1), the unordered structure is one in which $\nu = \nu_0$. In ‘dry’ proteins, the value for this structure is 1657 cm⁻¹ (Yang et al., 1987). In solution, a similar value is obtained for the H₂O medium while it shifts to 1643 cm⁻¹ in D₂O medium, reflecting peptide-to-solvent hydrogen bonding. Confusion can arise if only studies in D₂O are made, since bands in this region not due to unordered structure have been described in proteins.

4. Structure and function of membrane proteins

4.1. Cytochrome *c* oxidase

Respiratory cytochrome *c* oxidases are membrane proteins that reduce dioxygen into water. They are found in all three domains of life: eukaryotes, eubacteria and archaea (Castresana et al., 1994; Garcia-Horsman et al., 1994). The reduction of O₂ is mainly catalysed by a superfamily of enzymes, the haem–copper oxidases, which are structurally and functionally related. They typically contain a binuclear haem (Fe_{a3})–copper (Cu_{II}) centre to which the O₂ is bound, and where it is reduced to water by electron and proton transfer. The crystal structure of the mitochondrial (Tsukihara et al., 1996) and *P. denitrificans* (Iwata et al., 1995) enzymes of the *aa*₃-type subclass of cytochrome *c* oxidases has been obtained. They have three homologous core polypeptides called subunits I, II and III. The active site of the enzyme, a spin-coupled haem–copper centre, is located in subunit I, which contains 12 transmembrane segments. This subunit also houses the low-spin haem that is the electron donor to the active site. Subunit II has only two transmembrane spans, and most of it is located on the periplasmic side of the bacterial cell membrane. It is the latter, largely β-sheet domain the one that carries the electron entry site of the enzyme, the Cu_A-site.

The structure of the different cytochrome *c* oxidases was studied by infrared spectroscopy in eukaryotic (Caughey et al., 1993) and prokaryotic (Arrondo et al., 1994; Echabe and Arrondo, 1995; Echabe et al., 1995) enzymes, prior to the knowledge of the crystal structure. The information obtained was not only relevant to the secondary structure of the proteins, but also to the role and interactions of the different subunits. In contrast to subunits I and II, no well-defined role has been assigned for subunit III, which has no redox-active groups. Active two-polypeptide oxidases have been isolated from *P. denitrificans* either by depletion of subunit III or from a mutant devoid of subunit III gene (Hendler et al., 1991; Haltia et al., 1994). However, in the absence of subunit III the membrane-bound oxidase is partially inactive and

Table 1

Values corresponding to band position and percentage area obtained after decomposition of the amide I band in D₂O medium of cytochrome *c* oxidase from bovine heart mitochondria (Bcox), wild type *Paracoccus denitrificans* (Pcox) and a mutant of *P. denitrificans* lacking subunit III (Pcox_{III}⁻). The values are rounded off to the nearest integer

Bcox		Pcox		Pcox _{III} ⁻	
Band position	% Area	Band position	% Area	Band position	% Area
1693	< 1				
1682	5	1686	3	1685	3
1672	6	1674	10	1673	9
1658	39	1658	44	1658	42
1646	22	1644	24	1643	32
1636	15	1630	18	1628	15
1624	14				

heterogeneous (Haltia et al., 1989). Two point mutations in subunit III have been reported to be linked to a pathologic condition (Johns and Neufeld, 1993). The role of subunit III has been studied by comparing the wild strain (pCOX_{wt}) of cytochrome *c* oxidase from *P. denitrificans* with a mutant lacking subunit III (pCOX_{III}). The band decomposition of amide I in D₂O buffer for the mitochondrial cytochrome *c* oxidase and the two strains of *P. denitrificans* is shown in Table 1.

Interpretations of the differences between the wild type and mutant proteins based on percentage area changes are difficult because of the different number of amino acids involved in each protein. Hence, parameters less affected by multiple alterations were used in order to obtain information on the changes produced in individual components. Band area ratios (Table 2) isolate two components and make them comparable between both samples. The ratio α -helix/ β -sheet (1658/1630) is constant in pCOX_{wt} and pCOX_{III} implying that these two conformations do not vary in relation to each other when subunit III is not present. However, differences are seen in the ratios involving loops, unordered structure or β -turns. To ensure that a constant band ratio does not arise from a simultaneous change in the two bands involved, absolute areas can be ratioed to an internal reference (a nonconformational band, e.g. an aminoacid side chain band). Tyrosine C–C ring stretching vibration located at 1515 cm⁻¹ gives rise to an isolated band in the D₂O spectrum that is useful for this purpose. Fig. 5 shows the spectra of wild type and mutant cytochrome *c* oxidase in the 1800–1500 cm⁻¹ region in which the tyrosine band and the amide I components are shown. The ratio of component area vs. the 1515 cm⁻¹ band area (normalized to the number of tyrosines, 46 in the wild type enzyme and 36 in the mutant) is shown in Table 2. It can be seen that whereas the bands at around 1658 and 1630 cm⁻¹, related to α -helix and β -sheet, keep a constant ratio, the band around 1640 cm⁻¹, related to loops and unordered conformation, changes considerably. A smaller increase is observed in the value of the 1670+1680 cm⁻¹ bands, related to β -turns. Thus, it can be concluded that the α -helix and β -sheet structures are preserved in the mutant in the absence of subunit III, whereas unordered structure, loops and β -turns are affected by the loss of this subunit.

Table 2

Area ratios of band components of cytochrome *c* oxidase amide I band, and the normalized area of C–C Tyr ring vibration at 1515 cm⁻¹. Spectra taken in D₂O buffer. Adapted from (Echabe and Arrondo, 1995)

Band area ratio ^a	Assignment	Wild	Mutant
1658/1644	(α /loops + unordered)	2.03	1.15
1658/1630	(α / β)	2.18	2.15
1630/1644	(β /loops + unordered)	0.93	0.53
1658/1670 + 1680	(α /turns)	3.8	2.8
1658/Tyr	(α)	1.99	2.08
1644/Tyr	(loops + unordered)	1.07	1.88
1630/Tyr	(β)	0.93	0.95
1670 + 1680/Tyr	(turns)	0.58	0.72

^a Band positions are approximate, since they differ slightly between the wild type and mutant enzyme.

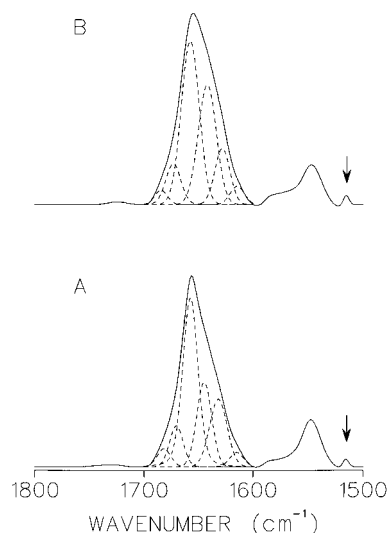


Fig. 5. The 1800–1500 cm^{-1} region of the wild type (A) and mutant (B) cytochrome *c* oxidase from *P. denitrificans* in D_2O medium showing the amide I band and the tyrosine C–C ring stretching band (arrow). Both have been fitted to their components. The spectra have been baseline corrected using a spline curve. Adapted from Echabe and Arrondo (1995).

Additional information on the interaction between subunit III and I+II can be obtained from thermal denaturation profiles. Fig. 6 shows the 3D-plots of pCOX_{wt} and pCOX_{III} cytochrome *c* oxidases. It can be seen that whereas the wild type enzyme exhibits two thermal transitions the mutant has only one, corresponding to the second endotherm observed with the wild enzyme. A more detailed profile can be obtained by plotting the positions of the bands corresponding to α -helix ($\approx 1657 \text{ cm}^{-1}$) and β -sheet ($\approx 1630 \text{ cm}^{-1}$) (Fig. 7). For comparison, the profiles corresponding to the mitochondrial enzyme, which has a highly cooperative profile, have been included. It can be shown that in the *P. denitrificans* enzyme whereas the α -helical element has a three-step denaturation in the wild type, the mutant exhibits only the denaturation associated to subunits I+II. Also noteworthy is the different behaviour of the β -sheet (extramembraneous) and the α -helix (mainly intramembraneous) components versus the thermal challenge. The thermal event producing this intermediate state involves a fraction of the subunit III, which is mainly α -helical (Haltia et al., 1994). Therefore, it can be said that two kinds of α -helices exist in subunit III, differing in their thermal response, which suggests that some of the subunit III helices have an anomalously unstable native state. Confirming these results, the crystal structure indicates that the helices in subunit III exist in two populations with different orientations. Thus, the picture obtained from infrared spectroscopy band decomposition is that the presence of subunit III does not produce changes in the transmembrane segments, i.e. in the haem–copper nuclei, but its absence alters the correct folding in the outer loops of subunit I+II. The oxygen-reducing activity of the oxidase is conserved in the protein lacking subunit III, but the activity is lost during the steady-state catalysis, and cannot be restored by introducing additional oxygen, opposite to the behaviour

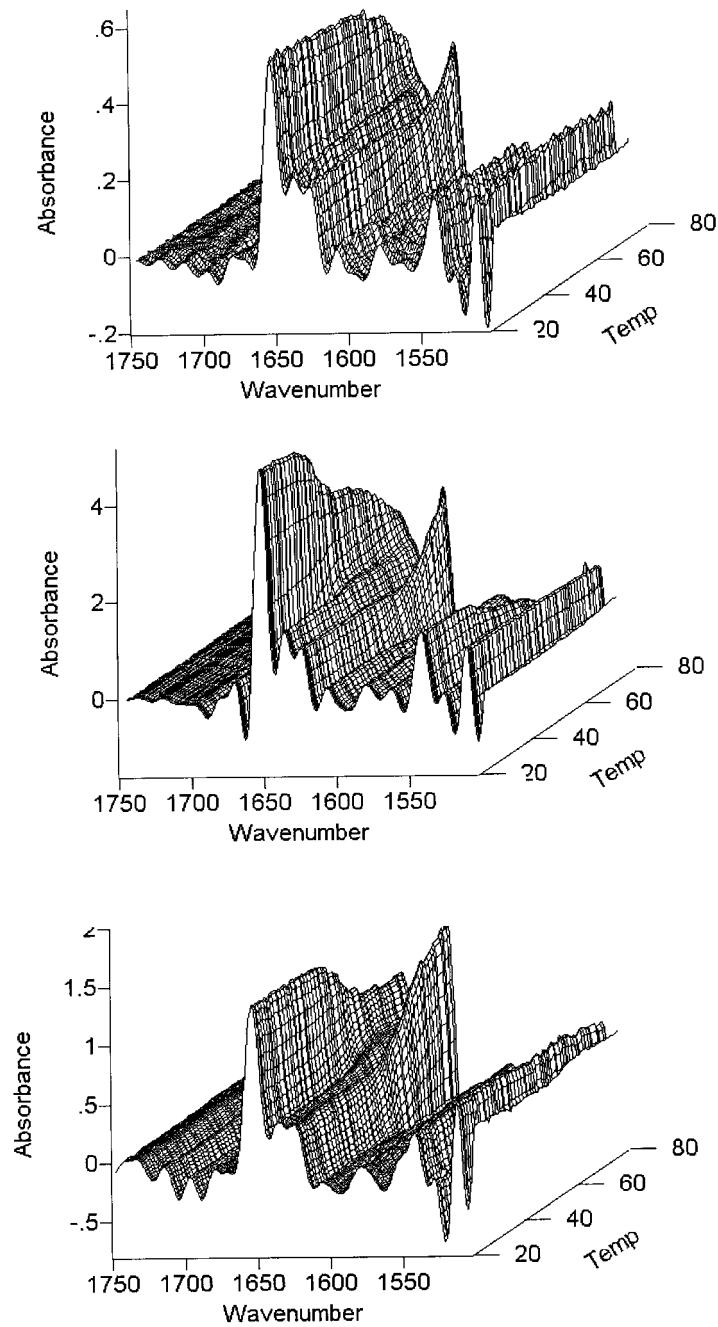


Fig. 6. 3D plots of absorbance/wavenumber (cm^{-1})/temperature of cytochrome *c* oxidase from bovine heart mitochondria (lower trace), from wild type *P. denitrificans* (medium trace), and from a *P. denitrificans* mutant lacking subunit III (upper trace).

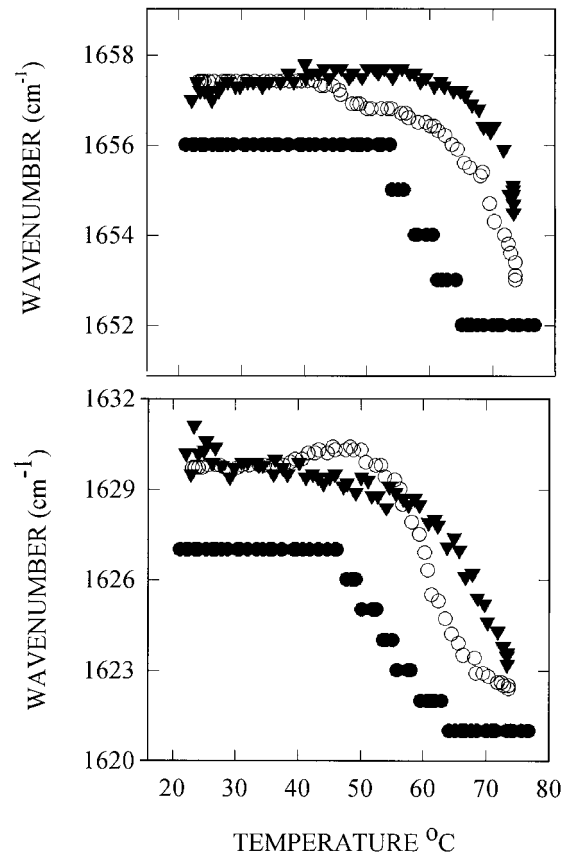


Fig. 7. Thermal profiles corresponding to the 1657 cm^{-1} band, corresponding to α -helix, and the 1630 cm^{-1} band, corresponding to β -sheet, of the cytochrome *c* oxidase from bovine heart mitochondria (●), wild type *P. denitrificans* (○), and a mutant of *P. denitrificans* lacking subunit III (∇).

of the protein with subunit III (Haltia et al., 1994). These findings have been confirmed by difference spectroscopy. According to this technique, the oxidized minus reduced spectra in anaerobic conditions of the pCOX_{wt} and $\text{pCOX}_{\text{III}^-}$ are identical indicating that the haem-copper nuclei are not affected by the absence of subunit III (Hellwig et al., 1998). From the crystal structure and mutagenesis studies, it has also been inferred that subunit III plays a special function in O_2 transport (Riistama et al., 1996). More recently, it has been shown in *R. spheroides* depleted of subunit III that this subunit is required to stabilize the structure of subunits I and II (Bratton et al., 1999). Here, it can be concluded that the presence of subunit III is essential for the correct folding of the extramembranal portion of subunits I+II and the proper constitution of the dyoxygen channel.

The mechanism of cytochrome *c* oxidase involves the formation of an electrochemical membrane proton gradient that drives ATP synthesis coupled to oxygen reduction. Besides the four protons required for water formation (termed scalar protons), up to four protons are pumped across the membrane that contribute to the electrochemical proton gradient. Oxygen

binds to the binuclear haem–copper centre where it is reduced. Structural information from X-ray crystallography on the four-subunit cytochrome *c* oxidase from *P. denitrificans* (Iwata et al., 1995) and the mitochondrial thirteen-subunit enzyme (Tsukihara et al., 1996) has been obtained recently. The idea of a mechanism of proton transfer across the protein by hopping along charged polar residues and water molecules has gained considerable strength. In cytochrome *c* oxidase, several possible channels for proton translocation have been described (Michel et al., 1998; Mills and Ferguson-Miller, 1998; Wikstrom, 1998) and tested by site-directed mutagenesis and difference spectroscopy. In *P. denitrificans* two possible proton transfer pathways have been suggested. The shorter one, termed the K-pathway, leads to the binuclear centre through three highly conserved residues of subunit I (Lys354, Thr351 and Tyr280) plus the hydroxyl group of the haem a_3 hydroxyethylfarnesyl chain. The longer pathway, named the D-pathway involves in subunit I Asp124 at the entrance and six conserved polar residues (Asn199, Asn113, Asn131, Tyr35, Ser134 and Ser193) located around the so-called pore C; the proton would leave pore C and reach Glu278 to approach finally the binuclear site. In the bovine enzyme, a third pathway, the H channel, passing haem a_3 , has also been described. Moreover, the D channel has been seen as a dead end with no channel function (Yoshikawa et al., 1998). The difference between the bovine and bacterial cytochrome *c* oxidase would point to different mechanisms between two remarkably similar structures, with very similar biochemical or biophysical parameters (Gennis, 1998).

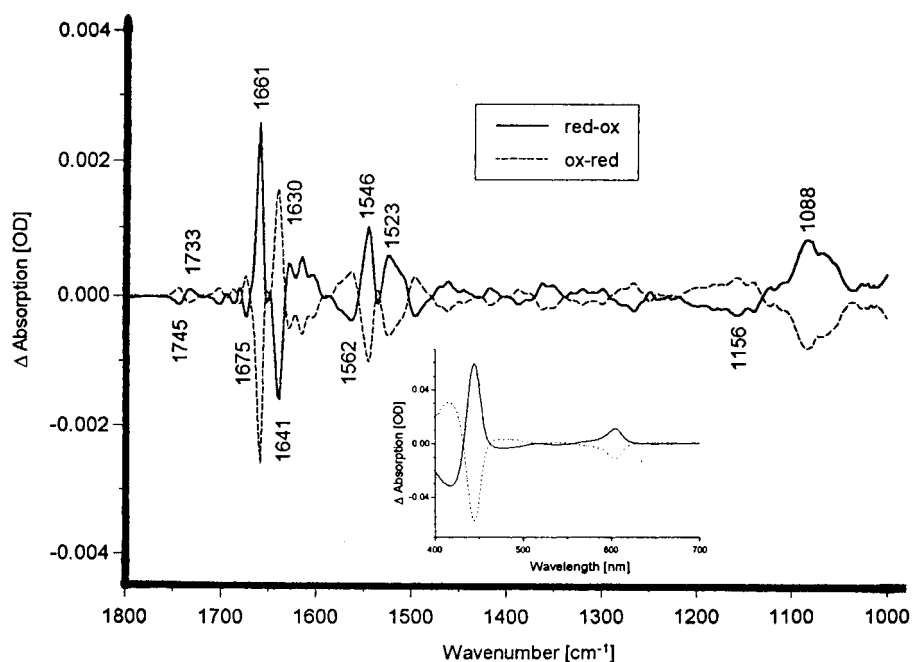


Fig. 8. Reduced-minus-oxidized (re-ox, full line) FTIR difference spectrum of cytochrome *c* oxidase obtained for a potential step from +0.5 to –0.2 V. The dashed–dotted line corresponds to the reverse difference spectrum obtained for a potential step from –0.2 to +0.5 V. Inset: difference spectrum obtained from the same sample in the visible spectral range. Adapted from Hellwig et al. (1996).

Difference spectroscopy has helped to understand the mechanisms of proton translocation by looking at the spectral changes produced during the reaction. Several approaches have been used to trigger the reaction and study the resulting spectral differences. Combination of several mutants with an ultra-thin-layer electrochemical cell in the absence of a ligand were used to obtain access to protein vibrational modes in the 1800–1000 cm^{-1} region, in order to examine protein function in the physiologically relevant states. The first results with the wild enzyme (Hellwig et al., 1996) showed highly structured band features with contributions mainly in the amide I and amide II, indicating structural rearrangements in the vicinity of the cofactor. The small amplitude of the IR difference signal suggests that these conformational changes are small and affect only individual peptide groups. In addition, a peak in the region above 1700 cm^{-1} , characteristic of the protonated side chain of Asp or Glu, was also found. The difference spectrum was reversible following the oxidation–reduction cycle (Fig. 8). A similar result was detected for *E. coli* cytochrome bo_3 using light activation of the ‘caged electron’ donor riboflavin (Lübber and Gerwert, 1996). Additional information was obtained by using mutants of Glu278 (Glu242 in the mitochondrial enzyme), a key residue in the D-pathway, together with a stepwise potential titration (Hellwig et al., 1998). The difference signal for the protonated carboxylic (Hellwig et al., 1996) group was resolved into two components and it was shown that Glu278 was involved in one of them. Mutation of Asp124 (Asp91 in the mitochondrial enzyme), another important residue in the D-pathway, does not change the difference spectrum.

Perturbing the *E. coli* cytochrome bo_3 by CO and studying the photodissociation of the transfer of the haem-bound CO to Cu_B in the binuclear site, also showed the involvement of the equivalent to Glu278 (Glu286) and correlated with Cu_B redox reactions (Puustinen et al., 1997). Besides, studying also the perturbation induced by CO in different mutants of the equivalent to Glu278 in *E. coli* cytochrome bo_3 , the proton connectivity of Glu with His was demonstrated together with the role of water in this connectivity (Riistama et al., 1997). Specific isotope labelling at the carboxyl groups of the four haem propionates has been used to study the involvement of these groups in proton translocation. Changes in the infrared difference spectrum can be correlated with variations in at least two of the four haem propionates, either by protonation/deprotonation or by environmental changes (Behr et al., 1998). Before the use of mutants became widespread, the binding and dynamics of ligands bound to the metal centres were used as probes for the changes in the haem-Cu centre (Caughey et al., 1993; Yoshikawa et al., 1995; Dodson et al., 1996).

4.2. Ca^{2+} -ATPase

Sarcoplasmic reticulum Ca^{2+} -ATPase is an integral protein that pumps calcium out of the cytoplasm during striated muscle relaxation (Martonosi, 1996). This is a P-type ATPase whose structure has been solved at 8 Å resolution by electron cryocrystallography (Zhang et al., 1998). The P-type ATPases are a family of transmembrane ion pumps primarily involved in the ATP hydrolysis-dependent transmembrane movement of a variety of inorganic cations against a concentration gradient, and having in common ten predicted transmembrane helical segments (Stokes et al., 1994). The structure and function of this membrane protein of unknown atomic structure has also been studied by infrared spectroscopy.

The structure of sarcoplasmic reticulum Ca^{2+} -ATPase has been predicted from the amino acid sequence (MacLennan et al., 1985) and modified after electron microscopy studies. The protein appears to consist of an extensive beak-shaped cytoplasmic domain containing interconnected α -helical and β -strand segments, a stalk connecting the beak with the membrane, and the ten transmembrane segments characteristic of P-type ion pumps (Kuhlbrandt et al., 1998). The cytoplasmic domain contains the active sites of ATP hydrolysis and phosphorylation while the Ca^{2+} channel is expected to be associated to the transmembrane domain. The Ca^{2+} -binding site is probably reached through a large cavity within the transmembrane domain. Comparing structures of Ca^{2+} -ATPase with and without bound nucleotide, it has been suggested that the ATP binding site is located in the cytoplasmic portion of the protein, and by using proteases a resistant domain has been isolated that is able to bind ATP (Champeil et al., 1998). Different experimental approaches, such as susceptibility of protein domains to protease digestion or changes in the interaction between protomers to form oligomeric structures, have been undertaken in order to understand the structural changes that link protein phosphorylation to cation translocation. Also, the quaternary structure of the pump is still undefined. Although it is generally accepted that the ATPase molecules form dimers and/or higher oligomers, monomeric Ca^{2+} -ATPase molecules are capable of performing all the steps of the reaction cycle (Andersen, 1989).

The structure of Ca^{2+} -ATPase has been investigated by infrared spectroscopy, first in a qualitative way, looking at the changes induced by different ligands that play a role in the kinetic mechanism of ATP-dependent Ca^{2+} translocation or lipid–protein interaction (Cortijo et al., 1982; Mendelsohn et al., 1984; Arrondo et al., 1985; Anderle and Mendelsohn, 1986; Arrondo et al., 1987; Buchet et al., 1990; Marcott et al., 1998). The secondary structure of Ca^{2+} -ATPase has also been obtained by decomposition of the amide I band (Villalaín et al., 1989; Himmelsbach et al., 1998) and by partial least squares analysis using a set of membrane proteins with known structures (Corbalán-García et al., 1994). These studies show a helical content of around 50% and ca. 20% β -sheet. Extensive proteolytic digestion of the protein removes the cytoplasmic domain and leads to a symmetric amide I band centred around 1656 cm^{-1} , indicating that the residual protein embedded in the membrane is α -helical (Corbalán-García et al., 1994), and confirming the predictions that the transmembrane protein segments of Ca^{2+} -ATPase are helices. Additional information can be obtained on the protein topology by analysis of the individual components or by using perturbing agents such as temperature. Ca^{2+} -ATPase has two noncanonical components in the amide I band (see the band assignment section), one is the component at 1645 cm^{-1} in the H_2O spectrum and the other is the 1625 cm^{-1} band in the D_2O spectrum. These bands cannot be unambiguously assigned and have been related to different structures such as 3_{10} -helix (Holloway and Mantsch, 1989), loops (Fabian et al., 1992) or more recently to coupled helical structures (Reisdorf and Krimm, 1996). Moreover, the band around 1625 cm^{-1} can be assigned to extended structures forming inter-molecular hydrogen bonds. In nondenatured proteins, this band has been assigned to protein–protein contacts (Martínez et al., 1996), thus pointing to the Ca^{2+} -ATPase as an oligomeric protein in the membrane.

Heat produces in many proteins an irreversible denaturation that is characterized in the infrared spectrum in D_2O buffer by the appearance of two bands, located at around 1620 and 1680 cm^{-1} , indicative of protein aggregation (Fabian et al., 1992; Arrondo et al., 1994). The

thermal profile of Ca^{2+} -ATPase does not correspond to a two-state denaturation, it rather shows an intermediate state characterized by changes in the noncanonical bands and β -sheet, but not in α -helix (Fig. 9). The combination of thermal and proteolytic studies allows a possible assignment of the band around 1645 cm^{-1} to cytoplasmic α -helical segments coupled to β -sheet (Himmelsbach et al., 1998). This tentative assignment has been later reinforced by different findings. Treatment of Ca^{2+} -ATPase with a variety of proteases results in the accumulation of a series of protease-resistant fragments that retain the ability to bind nucleotides and correspond to the cytoplasmic domain which contains the α/β structure (Champeil et al., 1998). Besides, the activity of Ca^{2+} -ATPase is inhibited in the presence of 3M urea and concomitantly, the thermal profile changes losing the intermediate state. Removal of urea leads to the recovery of both the activity and the thermal profile with an intermediate state (Fig. 10). These findings would point to a α/β domain stabilized by a special kind of interaction, that from the infrared data can be referred to as a coupling, that is needed for activity and presumably for nucleotide binding.

A further insight on the meaning of the band at 1645 cm^{-1} comes from a comparison of the 8 \AA structure of the Ca^{2+} -ATPase with other P-type ATPases such as *Neurospora* plasma membrane H^{+} -ATPase, that has also been solved at 8 \AA resolution (Auer et al., 1998). A

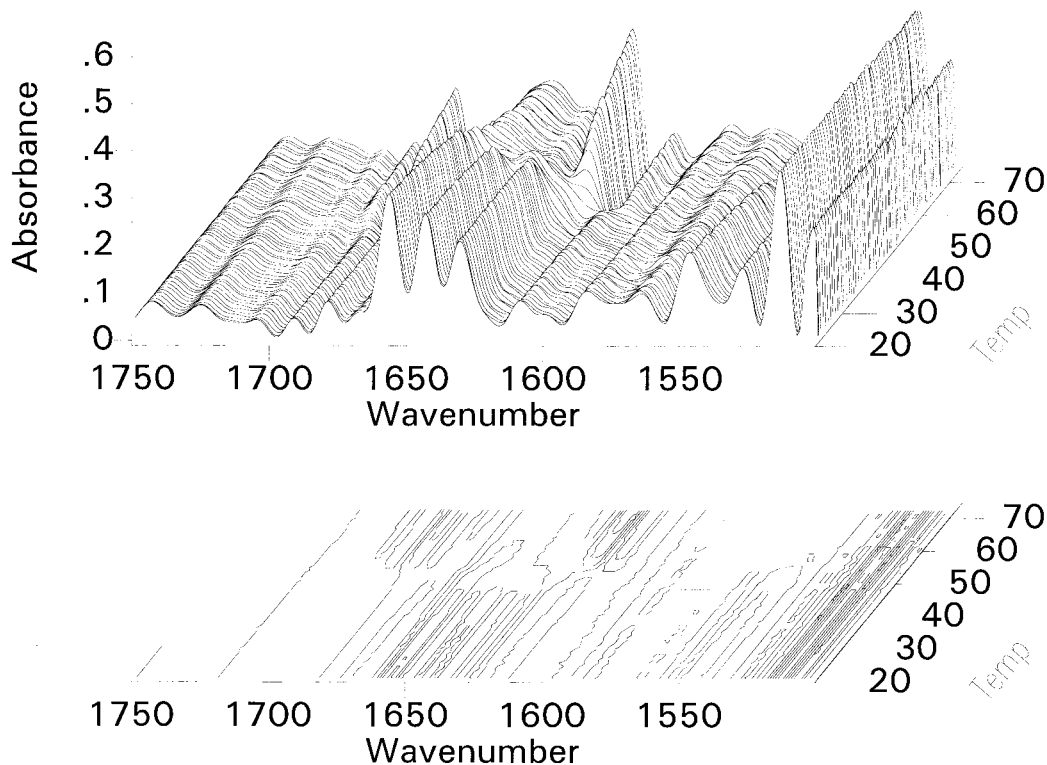


Fig. 9. 3D plot together with a 2D projection corresponding to the deconvolved spectra of Ca^{2+} -ATPase from sarcoplasmic reticulum from 20 to 80°C in the region $1800\text{--}1500\text{ cm}^{-1}$. The deconvolution parameters are $\text{FWHM} = 18\text{ cm}^{-1}$ and $k = 2.5$. The Z-axis corresponds to temperature.

comparison of both structures shows that the transmembrane helices are similar in both proteins, but the cytoplasmic regions appear to be significantly different. While the Ca^{2+} -ATPase region has a compact wedge shape, the cytoplasmic region of the H^{+} -ATPase has an open and cloven appearance (Kuhlbrandt et al., 1998). This result, that would be consistent with the more compact, coupled α/β domain in the Ca^{2+} -ATPase, is corroborated by the fact

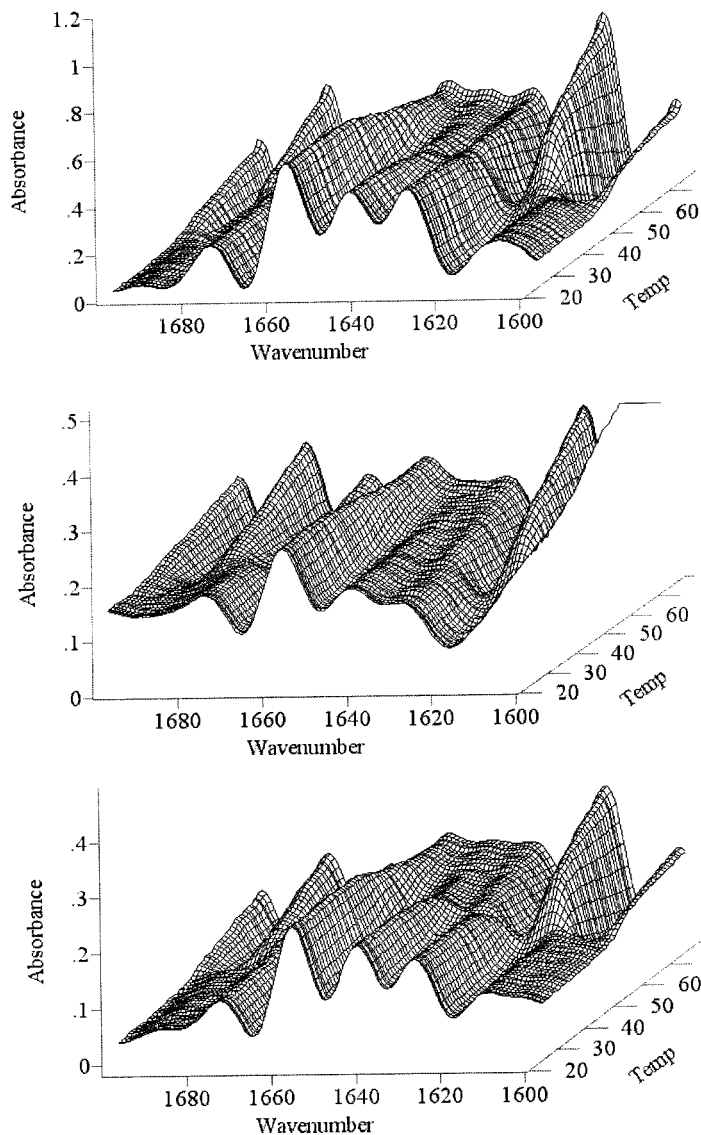


Fig. 10. Effect of 3 M urea on the infrared spectra of the amide I region of sarcoplasmic reticulum Ca^{2+} -ATPase in D_2O medium as a function of temperature. The protein is presented in the standard medium (lower trace), in the presence of 3 M urea (medium trace), and after having washed off the urea by centrifugation (upper trace). The spectra are deconvolved with a FWHH = 18 cm^{-1} and a $k2.5$.

that the infrared spectrum of the H^+ -ATPase lacks the band around 1645 cm^{-1} (Vigneron et al., 1995). Fig. 11 shows a comparison of the spectra of Ca^{2+} -ATPase and of gastric H^+ -ATPase, a P-type pump with an infrared spectrum very close to that of the *Neurospora crassa* plasma membrane H^+ -ATPase. Differences are also observed between Ca^{2+} -ATPase and gastric H^+ -ATPase when both proteins are subjected to partial proteolysis (Raussens et al., 1998b).

Ca^{2+} -ATPase transports calcium from the cytoplasm of muscle cells across the sarcoplasmic reticulum membrane, in a process that is essential for muscle relaxation. As in P-type ATPases, this transport is coupled to phosphorylation of an aspartic residue in a cycle that is depicted in Fig. 12. Ca^{2+} binds from the cytoplasmic side to high affinity sites located in the transmembrane domain yielding the Ca_2E_1 intermediate (step 1); ATP then phosphorylates the protein which occludes the bound Ca^{2+} ions and gives rise to the Ca_2E_1-P intermediate (step 2). Dissociation of calcium at the inner side of sarcoplasmic reticulum produces the E_2-P intermediate (step 3), and the cycle is closed by hydrolysis of the phosphoenzyme (step 4) and recovery of the resting form of the enzyme (for a review see Andersen and Vilsen, 1998). Early infrared work showed contradictory results between authors that found differences associated to the conformational intermediates involving α -helical structures (Arrondo et al., 1985; Arrondo et al., 1987) and those who did not find changes in protein structure that could be related to the reaction intermediates (Villalaín et al., 1989; Buchet et al., 1991).

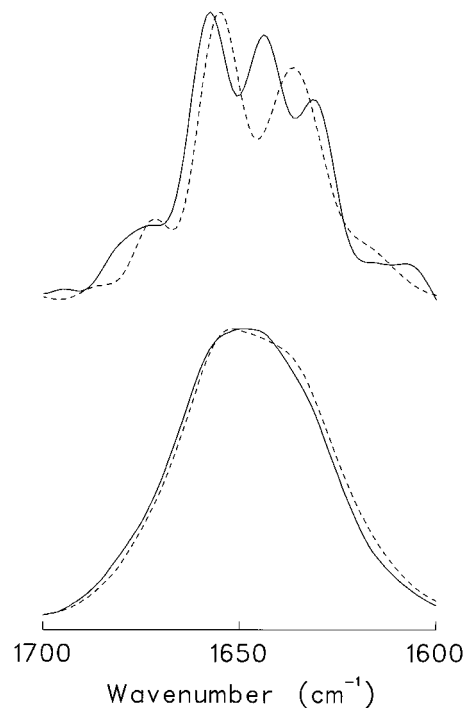


Fig. 11. Amide I region of the original (lower traces) spectra of sarcoplasmic reticulum Ca^{2+} -ATPase (solid line) and gastric H^+-K^+ -ATPase (dashed line) and the deconvoluted (upper traces) spectra of the same proteins. Deconvolution parameters are FWHH = 18 and $k2.25$.

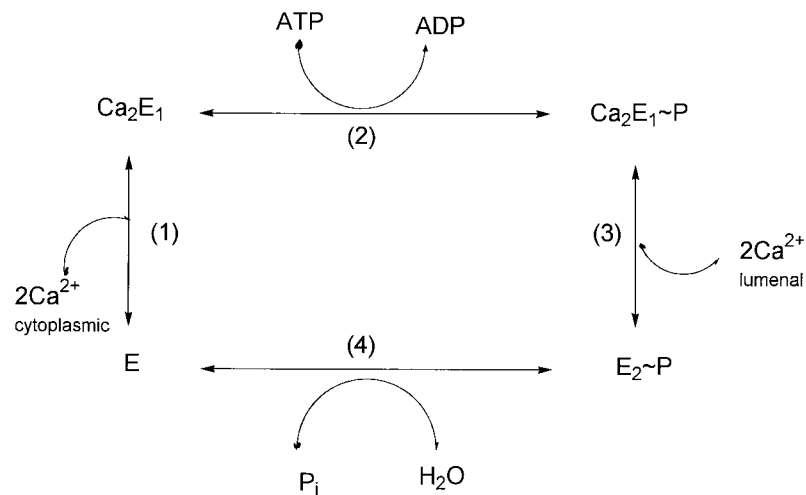


Fig. 12. Reaction scheme corresponding to the catalytic cycle of sarcoplasmic reticulum Ca²⁺-ATPase.

The possibility of using caged substrates, inactive photolabile compounds that are released by photolysis, made feasible the use of difference spectroscopy to study the reaction cycle with higher sensitivity. Two different substrates have been used to trigger the reaction, ATP and Ca²⁺. Caged ATP was used to study the different steps of the reaction cycle starting from the Ca₂E₁ intermediate and it was concluded that all reaction steps produced characteristic changes in the infrared spectrum, some of them in the amide I region. However, no outstanding conformational change was found associated to step 3, calcium release to the inner sarcoplasmic reticulum (Barth et al., 1994). A more detailed picture of the reaction cycle was obtained by using time-resolved difference infrared spectroscopy. The reaction steps can be temporally resolved, allowing the study of the different steps with the enzyme 'at work', not having to stop the reaction at the level of the different intermediates, but allowing the cycle to be completed (Barth et al., 1996). Using this method, it was shown that the difference spectrum of step 3 was almost identical to that of step 1 in the reaction cycle, implying that the same aminoacid residues would be involved in Ca²⁺ binding at the cytoplasmic or luminal sides. It was also proposed that upon Ca²⁺ release in the luminal side protons from that side would have access to the residues previously occupied by calcium (Barth et al., 1997).

A further study using caged ATP and [γ -¹⁸O₃]-caged ATP showed more clearly that the Ca²⁺ binding sites seem to be largely undisturbed by the phosphorylation reaction, that the phosphoenzyme phosphate group is unprotonated at pH 7.0 and that the C=O group of aspartyl phosphate does not interact with bulk water (Barth and Mantele, 1998). Previously, using caged Ca²⁺ as a trigger, the spectral changes produced by Ca²⁺ release, a positive band at 1650 cm⁻¹ and its negative side bands, had been interpreted as changes in step 2, so that phosphorylation would change the conformation induced by Ca²⁺ (Buchet et al., 1991). An additional recent work using caged Ca²⁺ as an effector of the reaction at low temperature also concluded that there were spectral changes associated to the Ca²⁺-triggered reaction cycle, involving changes in a band at 1653 cm⁻¹ attributable to α -helix, with small variations in

bands corresponding to other secondary structures; moreover, glutamic and/or aspartic acid side chains were deprotonated upon calcium binding (Troullier et al., 1996).

4.3. Nicotinic acetylcholine receptor

The nicotinic acetylcholine receptor (nAChR) is an intrinsic membrane protein that has been extensively studied by infrared spectroscopy. The structure, the effect of ligand binding and its interactions with the surrounding lipid have been observed. In this protein the effect of agonist and antagonist binding has been examined by amide I band analysis and difference spectroscopy. nAChR is the best characterized member of a family of ligand-gated ion channels involved mainly in neurotransmission. The structure of nAChR has been solved at 9 Å resolution both in the closed and open channel forms by electron microscopy (Unwin, 1998). Approximately half of the mass projects extracellularly beyond the lipid bilayer, about 30% corresponds to the transmembrane component and the remaining portion is in the cytoplasmic domain. It was suggested from the electron microscopy pictures that the transmembrane structure of the nAChR consisted of a ring of five α -helices surrounded by an electron dense component that could be attributed to β -sheet (Unwin, 1993).

Different studies on the secondary structure of the nAChR have been performed by infrared spectroscopy based on the analysis of the amide I band (Castresana et al., 1992; Butler and McNamee, 1993; Naumann et al., 1993; Méthot et al., 1995). The results suggest a helical content around 36–43%, and only one study gave a value of 19% (it must be stated that, as shown below, the helical content is highly dependent on the lipid composition of the reconstituted membranes). The β -sheet was first assigned to a band at 1639 cm^{-1} with a content of 48%; later, it was shown that this band also includes the unordered structure component (Martínez et al., 1996). Other authors found that the β -sheet structure was around 35–40%. The rest was unordered structure and turns. The transmembrane domain was investigated by removing the extracellular and intracellular sides of the membrane by proteolysis using proteinase K, with the result that after proteolytic treatment there was ca. 40% β -sheet structure and 50% α -helix, supporting the presence of β -sheet structure in the transmembrane domain (Görne-Tschelnokow et al., 1994). Other studies using hydrogen/deuterium exchange did not find an evidence of a large proportion of exchange-resistant peptides, which was interpreted as favouring the absence of β -sheet structure in the transmembrane domain (Baenziger and Méthot, 1995) and later a similar work was carried out with nAChR peptides containing one or more transmembrane segments (Corbin et al., 1998). More recently, it has been claimed that proteolysis under standard conditions does not remove all the extramembranal domain and that, with more extensive proteolysis after osmotic shock, an amide I band comparable to that of myoglobin is obtained, what is interpreted in support of the idea that the intramembranal domain is α -helical (Méthot and Baenziger, 1999).

Binding of cholinergic agonists to the appropriate binding sites on the extracellular domains of the nAChR elicits the formation of a transient cation channel, responsible for the initiation of postsynaptic membrane depolarisation. On continuous exposure to the agonist, however, the channel opening response becomes blocked and the affinity for the agonist increases, a process known as desensitisation. Introductory studies with membranes enriched in nAChR showed that prolonged exposure to cholinergic agonist, that drove the receptor into the desensitised

state, produced only negligible alterations in the amide I bandshape, but increased substantially the thermal stability of the protein. (Fernandez-Ballester et al., 1992). Using purified nAChR reconstituted in asolectin lipids the increased thermal stability seen upon cholinergic agonist binding is also observed, but in addition, changes in the amide I bandshape occur that are compatible with a loosening of the β -sheet structure upon reconstitution (Castresana et al., 1992). Using nAChR reconstituted in dioleoylphosphatidylcholine membranes only minor secondary structure changes were observed under conditions inducing desensitisation; however, variations in the lipid composition of the membranes used to reconstitute nAChR produced alterations in the secondary structure of the receptor (Butler and McNamee, 1993).

The significance of lipid–protein interactions in the structure and activity of nAChR was also put forward by a study on the effect of cholesterol. Reconstitution of the nAChR in lipidic vesicles in the absence of cholesterol results in a considerable loss of the ability of the receptor to support cation channel function. This functional loss is associated with the presence of specific lipids and is accompanied by changes in the amide I band resulting in an increase in the unordered structure and a decrease in the α -helical elements and the β -sheet. Adding increasing amounts of cholesterol up to the levels present in the native membranes, the amide I band recovers its shape and the overall secondary structure is also recovered (Table 3) (Fernandez-Ballester et al., 1994). The effect of neutral and anionic lipids was also studied by looking at the difference spectral pattern obtained in the different lipid environments in the presence or absence of an agonist. It was found that the main effect of both neutral and anionic lipids was to help stabilise nAChR in the resting conformation. The absence of neutral or anionic lipids leads nAChR into an alternative conformation similar to the one observed in the presence of the desensitising local anaesthetic, dibucaine (Ryan et al., 1996).

The effect of agonists on the structure and function of nAChR has also been studied by difference spectroscopy using either caged agonists or ATR in the presence or absence of agonists. Upon UV flash activation of a caged agonist analogue, spectral features were observed in the difference spectrum corresponding to both the agonist itself as well as to conformational changes of the receptor (Görne-Tschelnokow et al., 1992) in agreement with the changes observed in studies of the amide I band. A similar result was obtained using

Table 3

nAChR Area percentages of the amide I component bands obtained from curve-fitting the spectra corresponding to nAChR reconstituted in asolectin lipids (control), and in neutral lipid-depleted asolectin containing added cholesterol at 10, 20 and 40% molar. The component band at 1656 cm^{-1} corresponds to α -helix, the one at 1636 cm^{-1} to β -sheet plus random and the band at 1642 cm^{-1} to random plus loops

% Cholesterol	1656 cm^{-1} % area	1636 cm^{-1} (% area)	1642 cm^{-1} % area
0	32	40	20
10	34	45	15
20	35	43	13
40	44	50	0
Control	43	49	0

difference ATR, with variations in the sign and amplitude of the bands, what can be attributed to the different preparations used (Baenziger et al., 1992a,b; 1993). Further studies using hydrogen–deuterium exchange suggested that the formation of a channel-inactive desensitised state results predominantly from a conformational change in solvent-accessible extramembraneous regions of the polypeptide backbone (Méthot et al., 1995).

4.4. *Bacteriorhodopsin and related proteins*

Bacteriorhodopsin, a 26 kDa intrinsic membrane protein from *Halobacterium*, is the prototype of a protein family characterised by containing seven transmembrane helices. Some of its members, e.g. bacteriorhodopsin itself, contain retinal as a prosthetic group. Many proteins in this family, e.g. visual rhodopsin, are involved in signal transduction pathways via G proteins and constitute the group of the so-called ‘seven-helix receptors’ (G protein-coupled receptors, GPCR). The structure of bacteriorhodopsin and other seven-helix retinal proteins from halophilic bacteria has been reviewed recently (Oesterhelt, 1998). Two-dimensional crystals of bacteriorhodopsin, first studied in the primary work by Henderson and Unwin (1975), were resolved to 3.5 Å showing the classical seven-helix structure (Grigoriev et al., 1996) while further developments allowed the resolution of the structure at 3 Å by cryoelectron microscopy (Kimura et al., 1997). Later, the combination of synchrotron source development and microcrystals grown in lipid cubic phases provided a resolution by X-ray at 2.5 Å (Pebay-Peyroula et al., 1997) and 2.3 Å (Luecke et al., 1998) corroborating the overall structure obtained by electron microscopy, although differences in loops and some side-chain conformations are found among the different structures proposed (Oesterhelt, 1998).

From the early studies with polarised IR spectroscopy (for a review see (Rothschild and Clark, 1979) it became clear that the intramembraneous portion of bacteriorhodopsin consisted of α -helical rods oriented more or less perpendicularly with respect to the plane of the membrane. These studies also revealed that the predominant IR spectral component of bacteriorhodopsin displayed a characteristic maximum of absorbance at ca. 1665 cm^{-1} , a frequency well above those typically associated to α -helix. The origin of this peculiar absorbance maximum has been the object of debate. It was first assigned by Rothschild to distortion in the structure of bacteriorhodopsin α -helix (Rothschild and Clark, 1979), in turn attributed by Krimm to a weaker than average hydrogen bond caused by a conformational change from an α_{I} to an α_{II} type helix. This would result in a lengthening of the hydrogen bond distance, but because these helices are sequestered within the phospholipid membrane, there are no solvent molecules available to form bifurcated hydrogen bonds with the backbone CO acceptors, thus the CO stretching force constant is larger than in the α_{I} -helix (Reisdorf and Krimm, 1996). Tamm and Tatulian (1997), in the light of a variety of IR studies of peptides and proteins in different organic solvents, conclude that the shift of the amide I signal can be attributed to more flexible and/or more stretched α -helices.

IR spectroscopy has been important in describing other significant aspects of bacteriorhodopsin structure, namely the extended hydrogen-bond network between the proton acceptor Asp85 and the proton donor Asp96 (Lanyi, 1998). Thermal stability and a pathway for thermal destabilisation of bacteriorhodopsin have also been studied by IR spectroscopy (Taneva et al., 1995; Cladera et al., 1992). Thermal denaturation in D_2O media appeared to

follow the steps of rearrangement of helical structures (with loss of the 1665 cm^{-1} signal), extensive deuterium exchange, and finally protein aggregation.

Although a detailed description of bacteriorhodopsin mechanism is not within the scope of this review, we must mention in this context the impressive series of works that have addressed this problem combining differential IR spectroscopy, site-directed mutagenesis, isotope-editing and H/D exchange. As a result of those studies, many essential details are known that are helping in the understanding of the proton transduction mechanism (see, e.g. (Braiman and Rothschild, 1988; and references therein; Dioumaev and Braiman, 1997; Siebert, 1997; Lanyi, 1998; Oesterhelt, 1998)). More recently, conformational changes in the peptide backbone of the protein have been observed in the early part of the photocycle by a combination of H/D exchange and a low-temperature difference IR spectra on a membrane reconstituted sample of bacteriorhodopsin (Kluge et al., 1998).

Difference IR spectroscopy has also been applied to the study of structure-function relationships in visual rhodopsin ((Siebert, 1995; and references therein; Maeda et al., 1997; Oesterhelt, 1998). Site-directed mutagenesis and difference spectroscopy have provided evidence for interaction between transmembrane helices 3 and 5, mediated by Glu122 and His 211 (Beck et al., 1998), whereas combination of specific isotopic labelling with difference spectroscopy has allowed to monitor the possible involvement of tyrosines in the photoactivation of rhodopsin (Delange et al., 1998).

4.5. Other membrane proteins

Other integral membrane proteins have also been studied, although less extensively, by infrared spectroscopy. Among the P-type ATPases, and besides the Ca^{2+} -ATPase from sarcoplasmic reticulum, two other proteins have been described. The plasma membrane H^{+} -ATPase from *Neurospora crassa* has been examined in hydrated films at different stages of the enzyme catalytic cycle (Goormaghtigh et al., 1994a). No difference larger than 2% was found in the α -helix or β -sheet content of the H^{+} -ATPase in different conformational states. However, a difference in the hydrogen/deuterium exchange was seen suggesting variations in the tertiary structure. Using H^{+} -ATPase reconstituted in soybean phospholipid bilayers, and subjecting it to proteolysis, the amount of protein remaining after hydrolysis represented about 43% of the intact molecule and the membrane domain displayed a typical α -helix and β -sheet absorption pattern (Vigneron et al., 1995). H^{+} -ATPase from *Saccharomyces cerevisiae* has been purified in its two forms, the activated A-ATPase from glucose-metabolising cells and the basal-level B-ATPase from cells with endogenous metabolism only (Tanfani et al., 1998). Analysis of the infrared spectra revealed a different exposure to solvent in both forms, which is confirmed by the exchange rate of the amide hydrogens. The thermal profiles showed a similar denaturation temperature and a decrease in denaturation temperature was obtained for both forms in the presence of the inhibitor diethylstilbestrol. Another P-type pump has been characterised by infrared spectroscopy, namely the gastric H^{+} - K^{+} -ATPase. The structures before and after proteolytic degradation have been studied showing that the secondary structure is 35% α -helix, 35% β -sheets, 20% turns and 15% random, what is compatible with the classical transmembrane structure of the 10 helices P-type pumps (Raussens et al., 1997). Further studies of the proteolytic fragment combining infrared spectroscopy with circular

dichroism did not exclude the possible presence of β -sheet structure in the transmembrane region (Raussens et al., 1998a).

Lung surfactant and its specific proteins SP-B and SP-C have also been explored by infrared spectroscopy. It was found that the different fractions of the surfactant exhibited distinct positions of the amide I band with little or no effect on the structure and mobility of the phospholipids (Knells et al., 1995). SP-C had a mostly α -helical structure both in the pure state and in the presence of lipids, whereas SP-B structure was a mixture of α -helical and disordered forms (Pastrana-Rios et al., 1995).

Phospholamban, a 52-residue integral protein that regulates calcium uptake into the cardiac sarcoplasmic reticulum, as well as its 27–28 residue carboxy-terminal transmembrane segment that anchors the protein to the membrane have been examined by ATR with native (Tatulian et al., 1995) and site-directed isotope-labelled (Ludlam et al., 1996) aminoacids. The structure was predominantly α -helical, 64–67% in the intact protein and 73–82% in the C-terminal fragment, with small fractions of β -sheet and random structures. Specific local secondary structures of phospholamban have been probed by incorporating ^{13}C at two positions in the protein backbone. The authors interpreted their data as residues 39 and 46 being α -helical, with an axial orientation that was approximately 30° relative to the membrane normal. The transmembrane cysteine residues have also been investigated with the result that the sulfhydryl groups of the three cysteines present in the transmembrane helices were hydrogen-bonded to an $i-4$ backbone carbonyl oxygen (Arkin et al., 1997).

The secondary structure of photosystem II reaction centers isolated from pea was examined by IR spectroscopy in H_2O , D_2O and dried films. 40% α -helix, 10% β -sheets, 14% β -strands (or extended chains), 17% turns, 15% loops and 3% unordered segments were found (De las Rivas and Barber, 1997). These data are consistent with the 13 transmembrane helices that had been predicted for this multiprotein complex. These values were more consistent with an analysis of the aminoacid hydrophobic pattern and with the current models of the architecture of PSII than a previous work based on factor analysis and a comparison with a set of soluble proteins that gave 67.2% (He et al., 1991) or 62.3% (Zhang et al., 1997) α -helix structure. Another study on the effect of polyamines on PSII estimated 47% α -helix and 18% β -sheet that became 37% α -helix and 29% β -sheet upon polyamine complexation (Bograh et al., 1997).

Infrared data are also available for a variety of other integral membrane proteins. Thus, the β -sheet transmembrane barrel porin exhibited an infrared spectrum typical of β -sheet (Nabedryk et al., 1988). Limited proteolysis of porin revealed two membrane-bound forms, namely an 'adsorbed' and an 'inserted' one; which form was found depended on the lipids used to reconstitute the porin and on the temperature (Rodionova et al., 1995). Aquaporins are integral membrane proteins that mediate the permeability to water molecules; by infrared spectroscopy, it was shown that aquaporin-1 was a highly helical protein with 42–48% α -helix. The helices were more tilted than those of bacteriorhodopsin and they underwent limited hydrogen/deuterium exchange (Cabiaux et al., 1997). Another work on aquaporin found that the hydrogen/deuterium exchange was very important, 80% of the peptide groups exchanged within 5 min after the exposure, what was consistent with the presence of an open aqueous pore within this protein structure (Haris et al., 1995).

The tetrameric K^+ -channel from *Streptomyces lividans* in a lipid bilayer was studied by ATR showing 43% α -helix and 25% β -sheet with a 43% of the backbone amide protons

exchangeable with deuterium (Wolkers et al., 1995). Monodisperse lactose permease was 80% α -helical and stably folded at 20°C, and was readily susceptible to deuterium exchange (Patzlaff et al., 1998). Reflectance infrared spectroscopy was used to study the structural conformation of α -crystallin membranes in heating-cooling-reheating cycles; during the heating process, the composition of α -helix, random coil and β -sheet decreased with temperature, the content of turns increased but the original structures were recovered after cooling (Lin et al., 1998). Calexcitin is a low molecular weight GTP and Ca^{2+} -binding protein, which is phosphorylated by protein kinase C during associative learning; the secondary structure obtained by infrared spectroscopy and circular dichroism gives one third in α -helix and one fifth in β -sheet. The secondary structure is dependent on calcium binding, which induces an increase in α -helical content and is independent on ionic strength (Ascoli et al., 1997). Diacylglycerol kinase is a 13.2 kDa protein that spans the cytoplasmic membrane three times and that has at least 90 of its 121 residues in α -helix with a topological arrangement in which three transmembrane helices are well-aligned with the membrane normal while two amphipatic helices are approximately parallel with the membrane plane (Sanders et al., 1996).

5. Concluding remarks

Although in its present state infrared spectroscopy cannot resolve whole protein structures at the atomic level, this technique is certainly an extremely powerful tool in the study of protein secondary and higher structures. Large, integral membrane proteins that pose serious technical problems for crystallisation, NMR or circular dichroism studies, are readily accessible to IR analysis. When Fourier-transform IR first became readily available in the early eighties, there was a burst of interest, with a large number of proteins being studied by this technique, although unfortunately the intrinsic difficulties of the technique became simultaneously apparent. In the past decade, a more sober approach has been adopted, and protein IR spectroscopy has found its applicability in essentially two fields in membranes, the study of protein structure and the detection of small conformational changes by difference spectroscopy. The results described in the above sections exemplify the usefulness of IR spectroscopy in those two areas.

At present, a number of trends may be detected that, in all likelihood, will prove useful very soon. Chief among them, although perhaps too obvious to be noticed, is the constant improvement in instrumentation and software. Perhaps only those who have witnessed the birth of the Fourier-transform era can appreciate the truth of that assertion. Even techniques, e.g. IR microscopy that, as mentioned in the main body of the review, have not found up to now its application in the area of membrane proteins, are of enormous interest in themselves, and may become relevant to our field in a near future. The same can be said of IR imaging. More immediate promise for protein studies present the two-dimensional IR techniques, of which some exciting results are already available. Several reflectance techniques that allow the study of oriented peptides and proteins under native conditions, avoiding particularly the danger of partial denaturation during sample desiccation onto inert surfaces, are becoming available and will certainly provide interesting information. Finally, the widespread application of protein engineering and site-directed mutagenesis provides not only the most direct insights

on structure–function relationship, but also makes feasible the isotope-editing of certain aminoacid residues, thus giving rise to a new dimension in the IR studies of proteins, allowing the specific study of a given aminoacid residue in protein–protein interactions. In parallel with this progress, or perhaps intertwined with it, is the advance of computer-based prediction methods for protein structure, which guide in a gradually safer way the mutagenesis efforts. The combined use of improved optical detection and sampling techniques, molecular biology methods, and computing applications, is certain to keep infrared going well into the coming century.

Acknowledgements

This work was supported by Universidad del País Vasco (G03/98), Basque Government (Ex98/10 and PI98/33) and DGICYT (PB96/0171). The authors are grateful to Dr. P.H. Axelsen, Dr. T. Keiderling and Dr. E. Goormaghtigh for their help during the preparation of this manuscript.

References

- Alvarez, J., Haris, P.I., Lee, D.C., Chapman, D., 1987. Conformational changes in concanavalin A associated with demetallization and a-methylmannose binding studied by Fourier transform infrared spectroscopy. *Biochim. Biophys. Acta* 916, 5–12.
- Anderle, G., Mendelsohn, R., 1986. Fourier-transform infrared studies of Ca-ATPase/phospholipid interaction: survey of lipid classes. *Biochemistry* 25, 2174–2179.
- Andersen, J.P., 1989. Monomer-oligomer equilibrium of sarcoplasmic reticulum Ca^{2+} -ATPase and the role of subunit interaction in the Ca^{2+} pump mechanism. *Biochim. Biophys. Acta* 988, 47–72.
- Andersen, J.P., Vilsen, B., 1998. Structure-function relationships of the calcium binding sites of the sarcoplasmic reticulum Ca^{2+} -ATPase. *Acta Physiol. Scand. Suppl.* 643, 45–54.
- Arkin, I.T., Adams, P.D., Brünger, A.T., Aimoto, S., Engelman, D.M., Smith, S.O., 1997. Structure of the transmembrane cysteine residues in phospholamban. *J. Membr. Biol.* 155, 199–206.
- Arrondo, J.L.R., Blanco, F.J., Serrano, L., Goñi, F.M., 1996. Infrared evidence of a β -hairpin peptide structure in solution. *FEBS Lett.* 384, 35–37.
- Arrondo, J.L.R., Castresana, J., Valpuesta, J.M., Goñi, F.M., 1994. The structure and thermal denaturation of crystalline and noncrystalline cytochrome oxidase as studied by infrared spectroscopy. *Biochemistry* 33, 11650–11655.
- Arrondo, J.L.R., Mantsch, H.H., Müllner, N., Pikula, S., Martonosi, A., 1987. Infrared spectroscopic characterization of the structural changes connected with the $E_1 E_2$ transitions in the Ca^{2+} -ATPase of sarcoplasmic reticulum. *J. Biol. Chem.* 262, 9037–9043.
- Arrondo, J.L.R., Muga, A., Castresana, J., Bernabeu, C., Goñi, F.M., 1989. An infrared spectroscopic study of β -galactosidase structure in aqueous solutions. *FEBS Lett.* 252, 118–120.
- Arrondo, J.L.R., Muga, A., Castresana, J., Goñi, F.M., 1993. Quantitative studies of the structure of proteins in solution by Fourier-transform infrared spectroscopy. *Prog. Biophys. Mol. Biol.* 59, 23–56.
- Arrondo, J.L.R., Urbaneja, M.A., Goñi, F.M., Macarulla, J.M., Sarzala, G., 1985. Protein conformational transitions in sarcoplasmic reticulum membrane. *Biochem. Biophys. Res. Commun.* 128, 1159–1163.
- Arrondo, J.L.R., Young, N.M., Mantsch, H.H., 1988. The solution structure of concanavalin A probed by FTIR spectroscopy. *Biochim. Biophys. Acta* 952, 261–268.
- Ascoli, G.A., Luu, K.X., Olds, J.L., Nelson, T.J., Gusev, P.A., Bertucci, C., Bramanti, E., Raffaelli, A., Salvadori, P., Alkon, D.L., 1997. Secondary structure and Ca^{2+} -induced conformational change of calexcitin, a learning-associated protein. *J. Biol. Chem.* 272, 24771–24779.

- Auer, M., Scarborough, G.A., Kuhlbrandt, W., 1998. Three-dimensional map of the plasma membrane H⁺-ATPase in the open conformation. *Nature* 392, 840–843.
- Axelsen, P.H., Citra, M.J., 1996. Orientational order determination by internal reflection infrared spectroscopy. *Prog. Biophys. Mol. Biol.* 66, 227–253.
- Baello, B.I., Pancoska, P., Keiderling, T.A., 1999. Enhanced protein secondary structure prediction accuracy using hydrogen exchange FTIR spectroscopy. *Biophys. J.* 76, A171.
- Baenziger, J.E., Méthot, N., 1995. Fourier transform infrared and hydrogen deuterium exchange reveal an exchange-resistant core of α -helical peptide hydrogens in the nicotinic acetylcholine receptor. *J. Biol. Chem.* 270, 29129–29137.
- Baenziger, J.E., Miller, K.W., Rothschild, K.J., 1992a. Incorporation of the nicotinic acetylcholine receptor into planar multilamellar films: characterization by fluorescence and Fourier transform infrared difference spectroscopy. *Biophys. J.* 61, 983–992.
- Baenziger, J.E., Miller, K.W., McCarthy, M.P., Rothschild, K.J., 1992b. Probing conformational changes in the nicotinic acetylcholine receptor by Fourier transform infrared difference spectroscopy. *Biophys. J.* 62, 64–66.
- Baenziger, J.E., Miller, K.W., Rothschild, K.J., 1993. Fourier transform infrared difference spectroscopy of the nicotinic acetylcholine receptor: evidence for specific protein structural changes upon desensitization. *Biochemistry* 32, 5448–5454.
- Bandekar, J., 1992. Amide modes and protein conformation. *Biochim. Biophys. Acta* 1120, 123–143.
- Barth, A., Mäntele, W., 1998. ATP-Induced phosphorylation of the sarcoplasmic reticulum Ca²⁺ ATPase: molecular interpretation of infrared difference spectra. *Biophys. J.* 75, 538–544.
- Barth, A., Kreutz, W., Mäntele, W., 1990. Molecular changes in the sarcoplasmic reticulum calcium ATPase during catalytic activity: a Fourier transform infrared (FTIR) study using photolysis of caged ATP to trigger the reaction cycle. *FEBS Lett.* 277, 147–150.
- Barth, A., Kreutz, W., Mäntele, W., 1994. Changes of protein structure, nucleotide microenvironment, and Ca²⁺-binding states in the catalytic cycle of sarcoplasmic reticulum Ca²⁺-ATPase: investigation of nucleotide binding, phosphorylation and phosphoenzyme conversion by FTIR difference spectroscopy. *Biochim. Biophys. Acta* 1194, 75–91.
- Barth, A., Kreutz, W., Mäntele, W., 1997. Ca²⁺ release from the phosphorylated and the unphosphorylated sarcoplasmic reticulum Ca²⁺-ATPase results in parallel structural changes: an infrared spectroscopic study. *J. Biol. Chem.* 272, 25507–25510.
- Barth, A., Von Germar, F., Kreutz, W., Mäntele, W., 1996. Time-resolved infrared spectroscopy of the Ca²⁺-ATPase: the enzyme at work. *J. Biol. Chem.* 271, 30637–30646.
- Baumruk, V., Pancoska, P., Keiderling, T.A., 1996. Predictions of secondary structure using statistical analyses of electronic and vibrational circular dichroism and Fourier transform infrared spectra of proteins in H₂O. *J. Mol. Biology* 259, 774–791.
- Beck, M., Sakmar, T.P., Siebert, F., 1998. Spectroscopic evidence for interaction between transmembrane helices 3 and 5 in rhodopsin. *Biochemistry* 37, 7630–7639.
- Behr, J., Hellwig, P., Mäntele, W., Michel, H., 1998. Redox dependent changes at the haem propionates in cytochrome *coxidase* from *Paracoccus denitrificans*: direct evidence from FTIR difference spectroscopy in combination with haem propionate ¹³C labeling. *Biochemistry* 37, 7400–7406.
- Bograh, A., Gingras, Y., Tajmir-Riahi, H.A., Carpentier, R., 1997. The effects of spermine and spermidine on the structure of photosystem II proteins in relation to inhibition of electron transport. *FEBS Lett.* 402, 41–44.
- Bour, P., Sopkova, J., Bednarova, L., Malon, P., Keiderling, T.A., 1997. Transfer of molecular property tensors in Cartesian coordinates: a new algorithm for simulation of vibrational spectra. *J. Comput. Chem.* 18, 646–659.
- Braiman, M.S., Rothschild, K.J., 1988. Fourier transform infrared techniques for probing membrane protein structure. *Ann. Rev. Biophys. Chem.* 17, 541–570.
- Bratton, M.R., Hoganson, C., Hamer, A.G., Hosler, J.P., 1999. Subunit III of cytochrome *c oxidase* stabilizes the structures of subunits I and II. *Biophys. J.* 76, A254–A254.
- Buchet, R., Carrier, D., Wong, P.T., Jona, I., Martonosi, A., 1990. Pressure effects on sarcoplasmic reticulum: a Fourier transform infrared spectroscopic study. *Biochim. Biophys. Acta* 1023, 107–118.
- Buchet, R., Jona, I., Martonosi, A., 1991. Ca²⁺ release from caged-Ca²⁺ alters the FTIR spectrum of sarcoplasmic reticulum. *Biochim. Biophys. Acta* 1069, 209–217.

- Butler, D.H., McNamee, M.G., 1993. FTIR analysis of nicotinic acetylcholine receptor secondary structure in reconstituted membranes. *Biochim. Biophys. Acta* 1150, 17–24.
- Byler, D.M., Susi, H., 1986. Examination of the secondary structure of proteins by deconvolved FTIR spectra. *Biopolymers* 25, 469–487.
- Cabiaux, V., Oberg, K.A., Pancoska, P., Walz, T., Agre, P., Engel, A., 1997. Secondary structures comparison of aquaporin-1 and bacteriorhodopsin: a Fourier transform infrared spectroscopy study of two-dimensional membrane crystals. *Biophys. J.* 73, 406–417.
- Cameron, D.G., Moffat, D.J., 1984. Deconvolution, derivation, and smoothing of spectra using Fourier transforms. *J. Testing Eval.* 12, 78–85.
- Cameron, D.G., Moffat, D.J., 1986. A generalized approach to derivative spectroscopy. *Appl. Spectrosc.* 41, 539–544.
- Carmona, P., Navarro, R., Hernanz, A. (Eds.), 1997. *Spectroscopy of Biological Molecules: Modern Trends*. Kluwer Academic Publishers, Dordrecht.
- Castresana, J., Muga, A., Goñi, F.M., Arrondo, J.L.R., 1988a. A study of triose phosphate isomerase by FTIR. In: Schmid, E.D., Schneider, F.W., Siebert, F. (Eds.), *Spectroscopy of Biological Molecules. New Advances*. J. Wiley & Sons, Chichester.
- Castresana, J., Muga, A., Arrondo, J.L.R., 1988b. The structure of proteins in aqueous solutions: an assessment of triose phosphate isomerase structure by Fourier-transform infrared spectroscopy. *Biochem. Biophys. Res. Commun.* 152, 69–75.
- Castresana, J., Fernandez-Ballester, G., Fernandez, A.M., Laynez, J.L., Arrondo, J.L.R., Ferragut, J.A., Gonzalez-Ros, J.M., 1992. Protein structural effects of agonist binding to the nicotinic acetylcholine receptor. *FEBS Lett.* 314, 171–175.
- Castresana, J., Lübben, M., Saraste, M., Higgins, D.G., 1994. Evolution of cytochrome oxidase, an enzyme older than atmospheric oxygen. *EMBO J.* 13, 2516–2525.
- Caughey, W.S., Dong, A., Sampath, V., Yoshikawa, S., Zhao, X-J., 1993. Probing heart cytochrome oxidase structure and function by infrared spectroscopy. *J. Bioenergy Biomemb.* 25, 81–91.
- Cepus, V., Ulbrich, C., Allin, C., Troullier, A., Gerwert, K., 1998. Fourier transform infrared photolysis studies of caged compounds. *Methods Enzymol.* 291, 223–245.
- Champeil, P., Menguy, T., Soulié, S., Juul, B., Gomez de Gracia, A., Rusconi, F., Falson, P., Denoroy, L., Henao, F., Le Maire, M., Moller, J.V., 1998. Characterization of a protease-resistant domain of the cytosolic portion of sarcoplasmic reticulum Ca^{2+} -ATPase. *J. Biol. Chem.* 273, 6619–6631.
- Chehin, R., Iloro, I., Marcos, M.J., Villar, E., Shnyrov, V.L., Arrondo, J.L.R., 1999. Thermal and pH-induced conformational changes of a beta-sheet protein monitored by infrared spectroscopy. *Biochemistry* 38, 1525–1530.
- Cladera, J., Galisteo, M.L., Sabes, M., Mateo, P.L., Padros, E., 1992. The role of retinal in the thermal stability of the purple membrane. *Eur. J. Biochem.* 207, 581–585.
- Colarusso, P., Kidder, L.H., Levin, I.W., Fraser, J.C., Arens, J.F., Lewis, E.N., 1998. Infrared spectroscopic imaging: from planetary to cellular systems. *Appl. Spectrosc.* 52, A106–A120.
- Corbalán-García, S., Teruel, J.A., Villalaín, J., Gómez-Fernández, J.C., 1994. Extensive proteolytic digestion of the $(\text{Ca}^{2+} + \text{Mg}^{2+})$ -ATPase from sarcoplasmic reticulum leads to a highly hydrophobic proteinaceous residue with a mainly α -helical structure. *Biochemistry* 33, 8247–8254.
- Corbin, J., Methot, N., Wang, H.H., Baenziger, J.E., Blanton, M.P., 1998. Secondary structure analysis of individual transmembrane segments of the nicotinic acetylcholine receptor by circular dichroism and Fourier transform infrared spectroscopy. *J. Biol. Chem.* 273, 771–777.
- Cortijo, M., Alonso, A., Gómez-Fernández, J.C., Chapman, D., 1982. Intrinsic protein–lipid interactions: infrared spectroscopic studies of gramicidin a, bacteriorhodopsin and Ca^{2+} -ATPase in biomembranes and reconstituted systems. *J. Mol. Biol.* 157, 597–618.
- De Jongh, H.H.J., Goormaghtigh, E., Ruyschaert, J.M., 1996. The different molar absorptivities of the secondary structure types in the amide I region: an attenuated total reflection infrared study on globular proteins. *Anal. Biochem.* 242, 95–103.
- De las Rivas, J., Barber, J., 1997. Structure and thermal stability of photosystem II reaction centers studied by infrared spectroscopy. *Biochemistry* 36, 8897–8903.
- Delange, F., Klaassen, C.H., Wallace-Williams, S.E., Bovee-Geurts, P.H., Liu, X.M., DeGrip, W.J., Rothschild,

- K.J., 1998. Tyrosine structural changes detected during the photoactivation of rhodopsin. *J. Biol. Chem.* 273, 23735–23739.
- Dioumaev, A.K., Braiman, S.M., 1997. Nano and microsecond time-resolved FTIR spectroscopy of the halorhodopsin photocycle. *Photochem. Photobiol.* 66, 755–763.
- Dodson, E.D., Zhao, X.J., Caughey, W.S., Elliott, C.M., 1996. Redox dependent interactions of the metal sites in carbon monoxide-bound cytochrome *c* oxidase monitored by infrared and UV/visible spectroelectrochemical methods. *Biochemistry* 35, 444–452.
- Dong, A., Caughey, W.S., 1994. Infrared methods for study of hemoglobin reactions and structures. *Methods Enzymol.* 232, 139–175.
- Dong, A., Huang, P., Caughey, W.S., 1990. Protein secondary structures in water from second-derivative amide I infrared spectra. *Biochemistry* 29, 3303–3308.
- Dousseau, F., Pezolet, M., 1990. Determination of the secondary structure content of proteins in aqueous solutions from their amide I and amide II infrared bands: comparison between classical and partial least-squares methods. *Biochemistry* 29, 8771–8779.
- Earnest, T.N., Herzfeld, J., Rothschild, K.J., 1990. Polarized Fourier transform infrared spectroscopy of bacteriorhodopsin: transmembrane alpha helices are resistant to hydrogen/deuterium exchange. *Biophys. J.* 58, 1539–1546.
- Echabe, I., Arrondo, J.L.R., 1995. Infrared studies of eukaryotic and prokaryotic cytochrome *c* oxidases. In: Merlin, J.C., Turrell, S., Huvenne, J.P. (Eds.), *Spectroscopy of Biological Molecules*. Kluwer Academic Publishers, Dordrecht, pp. 123–126.
- Echabe, I., Arrondo, J.L.R., 1997. Structural analysis of proteins by infrared spectroscopy. In: Pifat-Mrzljak, G. (Ed.), *Supramolecular Structure and Function 5*. Balaban Publishers, Rehovot, pp. 9–23.
- Echabe, I., Haltia, T., Freire, E., Goñi, F.M., Arrondo, J.L.R., 1995. Subunit III of cytochrome *c* oxidase influences the conformation of subunits I and II: an infrared study. *Biochemistry* 34, 13565–13569.
- Fabian, H., Naumann, D., Misselwitz, R., Ristau, O., Gerlach, D., Welfle, H., 1992. Secondary structure of streptokinase in aqueous solution: a Fourier transform infrared spectroscopic study. *Biochemistry* 31, 6532–6538.
- Fernandez-Ballester, G., Castresana, J., Arrondo, J.L.R., Ferragut, J.A., Gonzalez-Ros, J.M., 1992. Protein stability and interaction of the nicotinic acetylcholine receptor with cholinergic ligands studied by Fourier-transform infrared spectroscopy. *Biochem. J.* 288, 421–426.
- Fernandez-Ballester, G., Castresana, J., Fernandez, A.M., Arrondo, J.L.R., Ferragut, J.A., Gonzalez-Ros, J.M., 1994. A role for cholesterol as a structural effector of the nicotinic acetylcholine receptor. *Biochemistry* 33, 4065–4071.
- Flach, C.R., Brauner, J.W., Taylor, J.W., Baldwin, R.C., Mendelsohn, R., 1994. External reflection FTIR of peptide monolayer films in situ at the air/water interface: experimental design, spectra–structure correlations, and effects of hydrogen–deuterium exchange. *Biophys. J.* 67, 402–410.
- Fraser, R.D.B., MacRae, T.P., 1973. Infrared spectrophotometry. In: *Conformation in Fibrous Proteins and Related Synthetic Polypeptides*. Academic Press, New York, pp. 94–125.
- Fringeli, U.P., Günthard, Hs.H., 1981. Infrared Membrane Spectroscopy. In: Grell, E. (Ed.), *Membr. Spectrosc.* Springer, Berlin, pp. 270–332.
- Garcia-Horsman, J.A., Barquera, B., Rumbley, J., Ma, J., Gennis, R.B., 1994. The superfamily of haem-copper respiratory oxidases. *J. Bacteriol.* 176, 5587–5600.
- Gennis, R., 1998. Cytochrome *c* oxidase: one enzyme, two mechanisms? *Science* 280, 1712–1713.
- Goormaghtigh, E., Ruyschaert, J.M., 1990. Polarized attenuated total reflectance infrared spectroscopy as a tool to investigate the conformation and orientation of membrane components. In: Brasseur, R. (Ed.), *Molecular Description of Biological Membranes by Computer Aided Conformational Analysis*, vol. I. CRC Press, Boca Raton, pp. 285–329.
- Goormaghtigh, E., Vigneron, L., Scarborough, G.A., Ruyschaert, J.-M., 1994a. Tertiary conformational changes of the *Neurospora crassa* plasma membrane H^+ -ATPase monitored by hydrogen/deuterium exchange kinetics: a Fourier transform infrared spectroscopy approach. *J. Biol. Chem.* 269, 27409–27413.
- Goormaghtigh, E., Cabiaux, V., Ruyschaert, J.-M., 1994b. Determination of soluble and membrane protein structure by Fourier transform infrared spectroscopy. In: Hilderson, H.J., Ralston, G.B. (Eds.), *Physicochemical Methods in the Study of Biomembranes*. Plenum Press, New York and London, pp. 329–450.
- Goormaghtigh, E., De Meutter, J., Vanloo, B., Brasseur, R., Rosseneu, M., Ruyschaert, J.M., 1989. Evaluation of

- the secondary structure of apo B-100 in low-density lipoprotein (LDL) by infrared spectroscopy. *Biochim. Biophys. Acta* 1006, 147–150.
- Görne-Tschelnokow, U., Hucho, F., Naumann, D., Barth, A., Mäntele, W., 1992. Fourier transform infrared (FTIR) spectroscopic investigation of the nicotinic acetylcholine receptor (nAChR): investigation of agonist binding and receptor conformational changes by flash-induced release of caged carbamoylcholine. *FEBS Lett.* 309, 213–217.
- Görne-Tschelnokow, U., Strecker, A., Kaduk, C., Naumann, D., Hucho, F., 1994. The transmembrane domains of the nicotinic acetylcholine receptor contain α -helical and β structures. *EMBO J.* 13, 338–341.
- Grigoriev, N., Ceska, T.A., Downing, K.H., Baldwin, J.M., Henderson, R., 1996. Electron-crystallographic refinement of the structure of bacteriorhodopsin. *J. Mol. Biol.* 259, 393–421.
- Haltia, T., Finel, M., Harms, N., Nakari, T., Raitio, M., Wikström, M., Saraste, M., 1989. Deletion of the gene for subunit III leads to defective assembly of bacterial cytochrome oxidase. *EMBO J.* 8, 3571–3579.
- Haltia, T., Semo, N., Arrondo, J.L.R., Goñi, F.M., Freire, E., 1994. Thermodynamic and structural stability of cytochrome *c* oxidase from *Paracoccus denitrificans*. *Biochemistry* 33, 9731–9740.
- Haris, P.I., Chapman, D., Benga, G., 1995. A Fourier-transform infrared spectroscopic investigation of the hydrogen–deuterium exchange and secondary structure of the 28-kDa channel-forming integral membrane protein (CHIP28). *Eur. J. Biochem.* 233, 659–664.
- Haris, P.I., Chapman, D., 1996. Fourier transform infrared spectroscopic studies of biomembrane systems. In: Mantsch, H.H., Chapman, D. (Eds.), *Infrared Spectroscopy of Biomolecules*. Wiley-Liss, Inc, New York, pp. 239–278.
- Harrick, N.J., 1967. *Internal Reflection Spectroscopy*. Wiley/Interscience, New York.
- He, W.Z., Newell, W.R., Haris, P.I., Chapman, D., Barber, J., 1991. Protein secondary structure of the isolated photosystem II reaction centre and conformational changes studied by Fourier transform infrared spectroscopy. *Biochemistry* 30, 4552–4559.
- Hellwig, P., Behr, J., Ostermeier, C., Richter, O.M.H., Pfitzner, U., Odenwald, A., Ludwig, B., Michel, H., Mäntele, W., 1998a. Involvement of glutamic acid 278 in the redox reaction of the cytochrome *c* oxidase from *Paracoccus denitrificans* investigated by FTIR spectroscopy. *Biochemistry* 37, 7390–7399.
- Hellwig, P., Ostermeier, C., Michel, H., Ludwig, B., Mantele, W., 1998b. Electrochemically induced FTIR difference spectra of the two- and four-subunit cytochrome oxidase from *P. denitrificans* reveal identical conformational changes upon redox transitions. *Biochim. Biophys. Acta* 1409, 107–112.
- Hellwig, P., Rost, B., Kaiser, U., Ostermeier, C., Michel, H., Mäntele, W., 1996. Carboxyl group protonation upon reduction of the *Paracoccus denitrificans* cytochrome *c* oxidase: direct evidence by FTIR spectroscopy. *FEBS Lett.* 385, 53–57.
- Henderson, R., Unwin, N., 1975. Three-dimensional model of purple membrane obtained by electron microscopy. *Nature* 257, 28–32.
- Hendler, R.W., Pardhasaradhi, K., Reynafarje, B., Ludwig, B., 1991. Comparison of energy-transducing capabilities of the two and three-subunit cytochromes aa₃ from *Paracoccus denitrificans* and the 13-subunit beef heart enzyme. *Biophys. J.* 60, 415–423.
- Herzyk, E., Lee, D.C., Dunn, R.C., Bruckdorfer, K.R., Chapman, D., 1987. Changes in the secondary structure of apolipoprotein B-100 after Cu²⁺-catalysed oxidation of human low-density lipoproteins monitored by Fourier transform infrared spectroscopy. *Biochim. Biophys. Acta* 922, 145–154.
- Himmelsbach, D.S., Khalili, S., Akin, D.E., 1998. FTIR microspectroscopic imaging of flax (*Linum usitatissimum* L.) stems. *Cell. Mol. Biol.* 44, 99–108.
- Holloway, P.W., Mantsch, H.H., 1989. Structure of cytochrome b₅ in solution by Fourier-transform infrared spectroscopy. *Biochemistry* 28, 931–935.
- Iwata, S., Ostermeier, C., Ludwig, B., Michel, H., 1995. Structure at 2.8 Å resolution of cytochrome oxidase from *Paracoccus denitrificans*. *Nature* 376, 660–669.
- Jackson, M., Haris, P.I., Chapman, D., 1989. Conformational transitions in poly(L-lysine): studies using Fourier transform infrared spectroscopy. *Biochim. Biophys. Acta* 998, 75–79.
- Jackson, M., Haris, P.I., Chapman, D., 1991. Fourier transform infrared spectroscopic studies of Ca²⁺-binding proteins. *Biochemistry* 30, 9681–9686.

- Johns, D.R., Neufeld, M.J., 1993. Cytochrome *c* oxidase mutations in Leber hereditary optic neuropathy. *Biochem. Biophys. Res. Commun.* 196, 810–815.
- Kennedy, D.F., Crisma, M., Toniolo, C., Chapman, D., 1991. Studies of peptides forming 3_{10} - and α -helices and β -bend ribbon structures in organic solution and in model biomembranes by Fourier transform infrared spectroscopy. *Biochemistry* 30, 6541–6548.
- Kimura, Y., Vassilyev, D.G., Miyazawa, A., Kidera, A., Matsushima, M., Mitsuoka, K., Murata, K., Hirai, T., Fujiyoshi, Y., 1997. Surface of bacteriorhodopsin revealed by high-resolution electron crystallography. *Nature* 389, 206–211.
- Kluge, T., Olejnik, J., Smilowitz, L., Rothschild, K.J., 1998. Conformational changes in the core structure of bacteriorhodopsin. *Biochemistry* 37, 10279–10285.
- Knells, G., Ahmed, M.K., Das, R.M., Oulton, M.R., Mantsch, H.H., Scott, J.E., 1995. Fourier-transform infrared spectroscopic analysis of rabbit lung surfactant: subfraction-associated phospholipid and protein profiles. *Chem. Phys. Lipids* 77, 193–201.
- Krimm, S., Bandekar, J., 1986. Vibrational spectroscopy and conformation of peptides, polypeptides and proteins. *Adv. Prot. Chem.* 38, 181–364.
- Krimm, S., Dwivedi, A.M., 1982. Infrared spectrum of the purple membrane: clue to a proton conduction mechanism. *Science* 216, 407–408.
- Krimm, S., Reisdorf Jr., W.C., 1994. Understanding normal modes of proteins. *Faraday Discuss.* 99, 181–197.
- Kuhlbrandt, W., Auer, M., Scarborough, G.A., 1998. Structure of the P-type ATPases. *Curr. Opin. Struct. Biol.* 8, 510–516.
- Lanyi, J.K., 1998. Understanding structure and function in the light-driven proton pump Bacteriorhodopsin. *J. Struct. Biol.* 124, 164–178.
- Lee, D.C., Haris, P.I., Chapman, D., Mitchell, R.C., 1990. Determination of protein secondary structure using factor analysis of infrared spectra. *Biochemistry* 29, 502–512.
- Lewis, E.N., Levin, I.W., Crocombe, R.A., 1997. Applications of infrared imaging with a focal plane array detector and a step-scan FTIR spectrometer. *Mikrochimica Acta Suppl.* 14, 589–590.
- Lin, S.Y., Ho, C.J., Li, M.J., 1998. Thermal stability and reversibility of secondary conformation of α -crystallin membrane during repeated heating processes. *Biophys. Chem.* 74, 1–10.
- Lübber, M., Gerwert, K., 1996. Redox FTIR difference spectroscopy using caged electrons reveals contributions of carboxyl groups to the catalytic mechanism of haem-copper oxidases. *FEBS Lett.* 397, 303–307.
- Ludlam, C.F.C., Arkin, I.T., Liu, X.M., Rothman, M.S., Rath, P., Aimoto, S., Smith, S.O., Engelmann, D.M., Rothschild, K.J., 1996. Fourier transform infrared spectroscopy and site-directed isotope labeling as a probe of local secondary structure in the transmembrane domain of phospholamban. *Biophys. J.* 70, 1728–1736.
- Luecke, H., Richter, H.T., Lanyi, J.K., 1998. Proton transfer pathways in bacteriorhodopsin at 2.3 Å. *Science* 280, 1934–1937.
- MacLennan, D.H., Brandl, C.J., Korczak, B., Green, N.M., 1985. Amino acid sequence of a Ca^{2+} - Mg^{2+} -dependent ATPase from rabbit muscle deduced from its complementary DNA sequence. *Nature* 316, 696–700.
- Maeda, A., Kandori, H., Yamazaki, Y., Nishimura, S., Hatanaka, M., Chon, Y.S., Sasaki, J., Needleman, R., Lanyi, J.K., 1997. Intramembrane signalling mediated by hydrogen-bonding of water and carboxyl groups in bacteriorhodopsin and rhodopsin. *J. Biochem. (Tokyo)* 121, 399–406.
- Mäntele, W., 1993. Reaction-induced infrared difference spectroscopy for the study of protein function and reaction mechanisms. *Trends Biochem. Sci.* 18, 197–202.
- Marcott, C., Reeder, R.C., Paschalis, E.P., Tatakis, D.N., Boskey, A.L., Mendelsohn, R., 1998. Infrared microspectroscopic imaging of biomineralized tissues using a mercury-cadmium-telluride focal-plane array detector. *Cell. Mol. Biol.* 44, 109–115.
- Martínez, A., Haavik, J., Flatmark, T., Arrondo, J.L.R., Muga, A., 1996. Conformational properties and stability of tyrosine hydroxylase studied by infrared spectroscopy: effect of iron/catecholamine binding and phosphorylation. *J. Biol. Chem.* 271, 19737–19742.
- Martonosi, A.N., 1996. Structure–function relationships in the Ca^{2+} -ATPase of sarcoplasmic reticulum: facts, speculations and questions for the future. *Biochim. Biophys. Acta* 1275, 111–117.
- Mendelsohn, R., Anderle, G., Jaworsky, M., Mantsch, H.H., Dluhy, R.A., 1984. Fourier transform infrared spec-

- troscopy studies of lipid–protein interaction in native and reconstituted sarcoplasmic reticulum. *Biochim. Biophys. Acta* 775, 215–224.
- Méthot, N., Baenziger, J.E., 1999. Isolation of the transmembrane domain of the NAChR by proteolysis and characterization by SDS-PAGE and FTIR spectroscopy. *Biophys. J.* 76, A336.
- Méthot, N., Demers, C.N., Baenziger, J.E., 1995. Structure of both the ligand and lipid-dependent channel-inactive states of the nicotinic acetylcholine receptor probed by FTIR spectroscopy and hydrogen exchange. *Biochemistry* 34, 15142–15149.
- Michel, H., Behr, J., Harrenga, A., Kannt, A., 1998. Cytochrome *c* oxidase: structure and spectroscopy. *Ann. Rev. Biophys. Biomol. Struct.* 27, 329–356.
- Miick, S.M., Martinez, G.V., Fiori, W.R., Todd, A.P., Millhauser, G.L., 1992. Short alanine-based peptides may form 3_{10} -helices and not α -helices in aqueous solution. *Nature* 359, 653–655.
- Mills, D.A., Ferguson-Miller, S., 1998. Proton uptake and release in cytochrome *c* oxidase: separate pathways in time and space? *Biochim. Biophys. Acta* 1365, 46–52.
- Muga, A., Arrondo, J.L.R., Bellon, T., Sancho, J., Bernabeu, C., 1993. Structural and functional studies on the interaction of sodium dodecyl sulfate with β -galactosidase. *Arch. Biochem. Biophys.* 300, 451–457.
- Nabedryk, E., Garavito, R.M., Breton, J., 1988. The orientation of β -sheets in porin: a polarized Fourier transform infrared spectroscopic investigation. *Biophys. J.* 53, 671–676.
- Naumann, D., Schultz, C., Görne-Tschelnokow, U., Hucho, F., 1993. Secondary structure and temperature behavior of the acetylcholine receptor by Fourier transform infrared spectroscopy. *Biochemistry* 32, 3162–3168.
- Oesterhelt, D., 1998. The structure and mechanism of the family of retinal proteins from halophilic archaea. *Curr. Opin. Struct. Biol.* 8, 489–500.
- Pancoska, P., Kubelka, J., Keiderling, T.A. 1999. Novel use of a static modification of two-dimensional correlation analysis. I. Comparison of the secondary structure sensitivity of electronic circular dichroism, FTIR and Raman spectra of proteins. *Appl. Spectrosc.* 53, 655–665.
- Pastrana-Rios, B., Taneva, S., Keough, K.M.W., Mautone, A.J., Mendelsohn, R., 1995. External reflection absorption infrared spectroscopy study of lung surfactant proteins SP-B and SP-C in phospholipid monolayers at the air/water interface. *Biophys. J.* 69, 2531–2540.
- Patzlaff, J.S., Moeller, J.A., Barry, B.A., Brooker, R.J., 1998. Fourier transform infrared analysis of purified lactose permease: a monodisperse lactose permease preparation is stably folded, alpha-helical and highly accessible to deuterium exchange. *Biochemistry* 37, 15363–15375.
- Pebay-Peyroula, E., Rummel, G., Rosenbusch, J.P., Landau, E.M., 1997. X-ray structure of bacteriorhodopsin at 2.5 Å from microcrystals grown in lipid cubic phases. *Nature* 277, 1676–1681.
- Pierce, J.A., Jackson, R.S., Van Every, K.W., Griffiths, P.R., 1990. Combined deconvolution and curve fitting for quantitative analysis of unresolved spectral bands. *Anal. Chem.* 62, 477–484.
- Puustinen, A., Bailey, J.A., Dyer, R.B., Mecklenburg, S.L., Wikstrom, M., Woodruff, W.H., 1997. Fourier transform infrared evidence for connectivity between CuB and glutamic acid 286 in cytochrome *bo*₃ from *Escherichia coli*. *Biochemistry* 36, 13195–13200.
- Raussens, V., Ruyschaert, J.M., Goormaghtigh, E., 1997. Fourier transform infrared spectroscopy study of the secondary structure of the gastric H⁺, K⁺-ATPase and of its membrane-associated proteolytic peptides. *J. Biol. Chem.* 272, 262–270.
- Raussens, V., De Jongh, H., Pézolet, H., Ruyschaert, J.M., Goormaghtigh, E., 1998a. Secondary structure of the intact H⁺, K⁺-ATPase and of its membrane-embedded region: an attenuated total reflection infrared spectroscopy, circular dichroism and Raman spectroscopy study. *Eur. J. Biochem.* 252, 261–267.
- Raussens, V., le Maire, M., Ruyschaert, J.M., Goormaghtigh, E., 1998b. Secondary structure of the membrane-bound domains of H⁺, K⁺-ATPase and Ca²⁺-ATPase, a comparison by FTIR after proteolysis treatment of the native membranes. *FEBS Lett.* 437, 187–192.
- Reisdorf Jr., W.C., Krimm, S., 1994. Protein normal modes: calculation of spectroscopically reliable infrared bands. *Biophys. J.* 66, A373.
- Reisdorf Jr., W.C., Krimm, S., 1996. Infrared amide I' band of the coiled coil. *Biochemistry* 35, 1383–1386.
- Rial, E., Muga, A., Valpuesta, J.M., Arrondo, J.L.R., Goñi, F.M., 1990. Infrared spectroscopic studies of detergent-solubilized uncoupling protein from brown-adipose-tissue mitochondria. *Eur. J. Biochem.* 188, 83–89.
- Richardson, J.S., 1981. The anatomy and taxonomy of protein structure. *Adv. Prot. Chem.* 24, 167–339.

- Riistama, S., Puustinen, A., Garcia-Horsman, J.A., Iwata, S., Michel, H., Wikström, M., 1996. Channelling of dioxygen into the respiratory enzyme. *Biochimica Biophys. Acta* 1275, 1–4.
- Riistama, S., Hummer, G., Puustinen, A., Dyer, R.B., Woodruff, W.H., Wikström, M., 1997. Bound water in the proton translocation mechanism of the haem-copper oxidases. *FEBS Lett.* 414, 275–280.
- Rodionova, N.A., Tatulian, S.A., Surrey, T., Jahnig, F., Tamm, L.K., 1995. Characterization of two membrane-bound forms of OmpA. *Biochemistry* 34, 1921–1929.
- Rothschild, K.J., Clark, N.A., 1979. Anomalous amide I infrared absorption of purple membrane. *Science* 204, 311–312.
- Ryan, S.E., Demers, C.N., Chew, J.P., Baenziger, J.E., 1996. Structural effects of neutral and anionic lipids on the nicotinic acetylcholine receptor: an infrared difference spectroscopy study. *J. Biol. Chem.* 271, 24590–24597.
- Sanders, C.R., Czerski, L., Vinogradova, O., Badola, P., Song, D., Smith, S.O., 1996. *Escherichia coli* diacylglycerol kinase is an alpha-helical polytopic membrane protein and can spontaneously insert into preformed lipid vesicles. *Biochemistry* 35, 8610–8618.
- Siebert, F., 1995. Infrared spectroscopy applied to biochemical and biological problems. *Methods Enzymol.* 246, 501–528.
- Siebert, F., 1997. Monitoring the mechanism of biological reactions by infrared spectroscopy. *Mikrochim. Acta Suppl.* 14, 43–50.
- Silvestro, L., Axelsen, P.H., 1999. Fourier transform infrared linked analysis of conformational changes in annexin V upon membrane binding. *Biochemistry* 38, 113–121.
- Stokes, D.L., Taylor, W.R., Green, N.M., 1994. Structure, transmembrane topology and helix packing of P-type ion pumps. *FEBS Lett.* 346, 32–38.
- Surewicz, W.K., Leddy, J.J., Mantsch, H.H., 1990. Structure, stability and receptor interaction of cholera toxin as studied by Fourier-transform infrared spectroscopy. *Biochemistry* 29, 8106–8111.
- Susi, H., Byler, D.M., 1987. Fourier transform infrared study of proteins with parallel β -chains. *Arch. Biochem. Biophys.* 258, 465–469.
- Susi, H., 1969. Infrared spectra of biological macromolecules and related systems. In: Timasheff, S.N., Stevens, L. (Eds.), *Structure and Stability of Biological Macromolecules*. Dekker, New York, pp. 575–663.
- Sutherland, G.B.B.M., 1952. Infrared analysis of the structure of amino acids: polypeptides and proteins. *Adv. Prot. Chem.* 5, 291–318.
- Tamm, L.K., Tatulian, S.A., 1997. Infrared spectroscopy of proteins and peptides in lipid bilayers. *Q. Rev. Biophys.* 30, 365–429.
- Taneva, S.G., Caaveiro, J.M.M., Muga, A., Goñi, F.M., 1995. A pathway for the thermal destabilization of bacteriorhodopsin. *FEBS Lett.* 367, 297–300.
- Tanfani, F., Lapathitis, G., Bertoli, E., Kotyk, A., 1998. Structure of yeast plasma membrane H^+ -ATPase: comparison of activated and basal-level enzyme forms. *Biochim. Biophys. Acta* 1369, 109–118.
- Tatulian, S.A., Jones, L.R., Reddy, L.G., Stokes, D.L., Tamm, L.K., 1995. Secondary structure and orientation of phospholamban reconstituted in supported bilayers from polarized attenuated total reflection FTIR spectroscopy. *Biochemistry* 34, 4448–4456.
- Tomita, K.I., Rich, A., DeLozé, C., Blout, E.R., 1962. The effect of deuteration on the geometry of the α -helix. *J. Mol. Biol.* 4, 83–92.
- Torii, H., Tasumi, M., 1992a. Model calculations on the amide-I infrared bands of globular proteins. *J. Chem. Phys.* 96, 3379–3387.
- Torii, H., Tasumi, M., 1992b. Application of the three-dimensional doorway-state theory to analyses of the amide-I infrared bands of globular proteins. *J. Chem. Phys.* 97, 92–98.
- Troullier, A., Gerwert, K., Dupont, Y., 1996. A time-resolved Fourier transformed infrared difference spectroscopy study of the sarcoplasmic reticulum Ca^{2+} -ATPase: kinetics of the high-affinity calcium binding at low temperature. *Biophys. J.* 71, 2970–2983.
- Tsukihara, T., Aoyama, H., Yamashita, E., Tomizaki, T., Yamaguchi, H., Shinzawa-Itoh, K., Nakashima, R., Yaono, R., Yoshikawa, S., 1996. The whole structure of the 13-subunit oxidized cytochrome *c* oxidase at 2.8 Å. *Science* 272, 1136–1144.
- Unwin, N., 1993. Nicotinic acetylcholine receptor at 9 Å resolution. *J. Mol. Biol.* 230, 1101–1124.
- Unwin, N., 1998. The nicotinic acetylcholine receptor of the Torpedo electric ray. *J. Struct. Biol.* 121, 181–190.

- Vigneron, L., Ruyschaert, J.-M., Goormaghtigh, E., 1995. Fourier transform infrared spectroscopy study of the secondary structure of the reconstituted *Neurospora crassa* plasma membrane H⁺-ATPase and of its membrane-associated proteolytic peptides. *J. Biol. Chem.* 270, 17685–17696.
- Villalaín, J., Gómez-Fernández, J.C., Jackson, M., Chapman, D., 1989. FTIR spectroscopic studies on the secondary structure of the Ca⁺⁺-ATPase of sarcoplasmic reticulum. *Biochim. Biophys. Acta* 1080, 29–33.
- Wi, S., Pancoska, P., Keiderling, T.A., 1998. Predictions of protein secondary structures using factor analysis on Fourier transform infrared spectra: effect of Fourier self-deconvolution of the amide I and amide II bands. *Biospectroscopy* 4, 93–106.
- Wikstrom, M., 1998. Proton translocation by the respiratory haem–copper oxidases. *Biochim. Biophys. Acta.* 1365, 185–192.
- Wolkers, W.F., Haris, P.I., Pistorius, A.M.A., Chapman, D., Hemminga, M.A., 1995. FTIR spectroscopy of the major coat protein of M13 and Pfl in the phage and reconstituted into phospholipid systems. *Biochemistry* 34, 7825–7833.
- Yang, P.W., Mantsch, H.H., Arrondo, J.L.R., Saint-Girons, I., Guillou, Y., Cohen, G.N., Barzu, O., 1987. Fourier transform infrared investigation of the *Escherichia coli* methionine aporepressor. *Biochemistry* 26, 2706–2711.
- Yoshikawa, S., Mochizuki, M., Zhao, X.J., Caughey, W.S., 1995. Effects of overall oxidation state on infrared spectra of haem a₃ cyanide in bovine heart cytochrome c oxidase: evidence of novel mechanistic roles for Cu_B. *J. Biol. Chem.* 270, 4270–4279.
- Yoshikawa, S., Shinzawa-Itoh, K., Nakashima, R., Yaono, R., Yamashita, E., Inoue, N., Yao, M., Fei, M.J., Libeu, C.P., Mizushima, T., Yamaguchi, H., Tomizaki, T., Tsukihara, T., 1998. Redox-coupled crystal structural changes in bovine heart cytochrome c oxidase. *Science* 280, 1723–1729.
- Zhang, P.J., Toyoshima, C., Yonekura, K., Green, N.M., Stokes, D.L., 1998. Structure of the calcium pump from sarcoplasmic reticulum at 8-Å resolution. *Nature* 392, 835–839.
- Zhang, H.M., Yamamoto, Y., Ishikawa, Y., Zhang, W.L., Fischer, G., Wydrzynski, T., 1997. A Fourier transform infrared spectroscopic study of the effects of hydrogen peroxide and high light on protein conformations of photosystem II. *Photosynth. Res.* 52, 215–223.